



## Distribution and sources of organic matter in submarine canyons incising the Gulf of Palermo, Sicily: A multi-parameter investigation

Sarah Paradis<sup>1,2</sup>, Hannah Gies<sup>2</sup>, Davide Moccia<sup>3</sup>, Julie Lattaud<sup>2,4</sup>, Lisa Bröder<sup>2</sup>, Negar Haghypour<sup>2,5</sup>, Antonio Pusceddu<sup>3</sup>, Albert Palanques<sup>6</sup>, Pere Puig<sup>6</sup>, Claudio Lo Iacono<sup>6</sup>, and Timothy I. Eglinton<sup>2</sup>

<sup>1</sup>Environmental Physics, Institute of Biogeochemistry and Pollutant Dynamics, ETH Zurich, Zürich, Switzerland

<sup>2</sup>Geological Institute, ETH Zürich, Zürich, Switzerland

<sup>3</sup>Dipartimento di Scienze della Vita e dell'Ambiente, Università degli Studi di Cagliari, Cagliari, 09126, Italy

<sup>4</sup>Environmental Science department, Stockholm University, 11418, Stockholm, Sweden

<sup>5</sup>Laboratory for Ion Beam Physics, Department of Physics, ETH Zürich, 8093 Zürich, Switzerland

<sup>6</sup>Marine Sciences Institute, Consejo Superior de Investigaciones Científicas, Barcelona, 08003, Spain

**Correspondence:** Sarah Paradis (sparadis@ethz.ch)

Received: 2 June 2025 – Discussion started: 17 June 2025

Revised: 5 September 2025 – Accepted: 5 September 2025 – Published: 22 October 2025

**Abstract.** Submarine canyons act as conduits of terrigenous and marine organic carbon (OC) to deep-sea environments, although the contribution of each of these sources can largely vary depending on the canyon morphology and the prevailing sedimentary dynamics. The Gulf of Palermo is incised by several submarine canyons of similar dimension and depth range, but with slightly different morpho-sedimentary characteristics. Using a combination of geochemical parameters (OC, TN,  $\delta^{13}\text{C}$ ,  $\delta^{15}\text{N}$ , and  $\Delta^{14}\text{C}$ ), as well as biomarker signatures (proteins, carbohydrates, lipids, phytopygments, glycerol dialkyl glycerol tetraethers, and *n*-alkyl lipids) and compound-specific  $\delta^{13}\text{C}$  analyses of surficial sediments, we assess the sources of OC deposited on the shelf and in three major submarine canyons (Arenella, Oreto and Eleuterio canyons). The aim is to provide further insights on the role of submarine canyons in transporting terrigenous OC across continental margins. According to a dual isotopic end-member mixing model with  $\delta^{13}\text{C}$  and  $\Delta^{14}\text{C}$ , the contribution of terrigenous OC was highest on the shelf (80 %) and decreased offshore, with contributions that ranged between 50 % to 70 % across the studied canyons. The dispersal mechanism of terrigenous OC and its specific sources differ among canyons primarily because of local differences of hydro- and sediment dynamics. Arenella Canyon, which is up-current and farthest from any river mouth, exhibited the relatively lowest terrigenous OC contributions (50 %), Oreto Canyon in the central part of the gulf had slightly higher con-

tributions (50 %–70 %), and Eleuterio Canyon down-current and closest to shore had the highest proportion of terrigenous OC (60 %–70 %). Besides natural sediment dispersal mechanisms acting on this continental margin, continuous sediment resuspension by bottom trawling activities inside Oreto Canyon contributes to the down-canyon displacement of terrigenous OC, while promoting the ageing and degradation of OC in the canyon axis. Compound-specific  $\delta^{13}\text{C}$  analyses of fatty acids revealed that the sources of terrigenous OC differ across the studied submarine canyons, with Arenella and Oreto canyons receiving OC from a similar terrigenous source up-current from the gulf, whereas terrigenous OC deposited on the shelf and in Eleuterio Canyon originates from the Oreto and Eleuterio rivers that discharge into the Gulf of Palermo. This study provides further evidence that even non-river connected submarine canyons, such as Arenella, Oreto, and Eleuterio canyons in the Gulf of Palermo, are important sites of terrigenous OC sequestration and transfer to deep-sea environments, and that bottom trawling activities within submarine canyon environments can contribute to its resuspension and dispersal towards deeper regions.

## 1 Introduction

Continental margins are important sites of organic carbon (OC) accumulation, receiving inputs from both marine and terrigenous sources. The majority of terrigenous OC are deposited in estuaries and deltas or close to their riverine source, with limited transport of terrigenous OC to continental slopes and the deep-sea environments (Hedges and Keil, 1995; Burdige, 2005). However, efficient transfer of terrigenous particles and associated OC between continental shelves and deep-sea basins can be facilitated by submarine canyons. This transport is particularly important in river-connected canyons, which act as direct conduits of terrigenous riverine material into the canyon's interior (Huh et al., 2009; Baudin et al., 2020; Baker et al., 2024). Shelf-incising submarine canyons can also intercept materials entrained in along-margin sediment transport, funneling large volumes of terrigenous particles towards the canyon's interior (Puig et al., 2014). These high sediment fluxes and mass accumulation rates within submarine canyons lead to efficient marine and terrigenous OC sequestration within their interior (Masson et al., 2010; Maier et al., 2019; Baker et al., 2024), making these sites hotspots for OC burial.

As submarine canyons transport significant amounts of both marine and terrigenous OC to deep-sea environments, they also influence the benthic communities that inhabit these geomorphologic features (De Leo et al., 2010; Dell'Anno et al., 2013; Pusceddu et al., 2013; Fernandez-Arcaya et al., 2017; Campanyà-Llovet et al., 2018). The relative contributions of terrigenous and marine OC, where terrigenous OC tends to be less labile than marine OC, dictate the nutritional quality of the OC available to the benthos, thereby also affecting their abundance, biomass and diversity (Pusceddu et al., 2010; Gambi et al., 2014, 2017; Leduc et al., 2020). Higher marine OC tend to accumulate in submarine canyons incising continental margins with high marine primary productivity (Pusceddu et al., 2010), whereas the proportion of terrigenous OC in submarine canyons can be very variable depending on the proximity of riverine sources, their suspended sediment yield, and the magnitude of littoral and along-margin transport (Alt-Epping et al., 2007; Pasqual et al., 2013; Kao et al., 2014; Romero-Romero et al., 2016; Prouty et al., 2017; Gibbs et al., 2020). These contributions can also vary temporally, with enhanced sediment transport and burial of both marine and terrigenous OC triggered by natural energetic events such as storms, or by anthropogenic sediment resuspension and its posterior downcanyon transport caused by mobile demersal fisheries (Pedrosa-Pàmies et al., 2013; Liu et al., 2016; Paradis et al., 2022).

The relative contributions of terrigenous and marine OC can be determined using different approaches. The molar ratio of OC to total nitrogen (OC / TN) is often employed to distinguish between terrigenous and marine sources of OC (Gordon and Goñi, 2003; Ramaswamy et al., 2008). However, this ratio may undergo post-depositional alterations due

to the preferential degradation of nitrogen, which limits its reliability for determining the source of OC over longer timescales or in settings where significant degradative loss of organic matter (OM) occurs (Meyers, 1994; Briggs et al., 2013). The stable isotopic composition of OC ( $\delta^{13}\text{C}$ ) is widely used to identify sedimentary sources (Pedrosa-Pàmies et al., 2013; Wei et al., 2024), given the distinct signature of marine OC ( $-24\text{‰}$  to  $-20\text{‰}$ ; e.g., Verwege et al., 2021) and terrigenous OC, the latter depending on whether it is dominated by  $\text{C}_3$  ( $-32\text{‰}$  to  $-24\text{‰}$ ) or  $\text{C}_4$  ( $-16\text{‰}$  to  $-10\text{‰}$ ) plant inputs (e.g., Bender, 1971; Farquhar et al., 1989). However, mixed inputs of vegetation from a river basin can result in overlapping  $\delta^{13}\text{C}$  signatures, hindering apportionment of OC sources (Goñi et al., 1998; Gordon and Goñi, 2003). Although used less often, the isotopic composition of total nitrogen ( $\delta^{15}\text{N}$ ) can also help elucidate the contribution of terrigenous and marine OC deposited in marine sediments (Ramaswamy et al., 2008; Romero-Romero et al., 2016; Palanques and Puig, 2018). However,  $\delta^{15}\text{N}$  signatures can also be affected by diagenetic processes (Thornton and McManus, 1994; Lehmann et al., 2002), and overlapping  $\delta^{15}\text{N}$  values of terrigenous ( $-2\text{‰}$  to  $6\text{‰}$ ) and marine ( $2\text{‰}$  to  $6\text{‰}$ ) sources (Deegan and Garritt, 1997; Amundson et al., 2003) may further complicate source apportionment. Finally, the radiocarbon signature of OC ( $\Delta^{14}\text{C}$ ) can be coupled with  $\delta^{13}\text{C}$  values in dual end-member models in order to resolve the sources of OC deposited in marine sediments (e.g., Ausín et al., 2023; Kim et al., 2022). However, OC can age during its transport across the continental margin (Bao et al., 2016, 2019; Bröder et al., 2018; Paradis et al., 2024), while preferential degradation of younger, more labile components relative to older and more recalcitrant OC fractions (Kusch et al., 2021; Paradis et al., 2023) may further influence  $^{14}\text{C}$  signatures. However, these bulk-level analyses generally cannot be used to distinguish between specific sub-pools of terrigenous OC (e.g. vegetation, soils, and fossil OC).

Hence, these parameters need to be complemented with source-specific organic molecules (hereafter biomarkers) to confirm the OC source apportionment and to disentangle the different origins of terrigenous OM deposited in marine sediments. For example, lignin phenols can indicate the influence of terrigenous vegetation while distinguishing between contributions of different vascular plant types (Tesi et al., 2012; Goñi et al., 2013, 2014). In addition, there exist a wide range of lipids, such as glycerol dialkyl glycerol tetraethers (GDGTs) and *n*-alkyl lipids, that are specific to marine and different terrigenous sources. GDGTs are membrane lipids of archaea and bacteria found in marine and terrigenous environments, and they can either have isoprenoid (isoGDGTs) or branched (brGDGTs) structures (Koga et al., 1993; Sinninghe Damsté et al., 2000). BrGDGTs are generally found in soil bacteria, whereas isoGDGTs are common in marine archaea, with crenarchaeol often the most abundant isoGDGT in temperate environments (Sinninghe Damsté et al., 2002). However, a growing number of studies have shown

that brGDGTs can also be produced by bacteria in specific marine environments (Peterse et al., 2009; Zhu et al., 2011; Weijers et al., 2014; Sinnighe Damsté, 2016), so their application requires corroboration using complementary proxies (Sinnighe Damsté, 2016; Xiao et al., 2016).

The composition of *n*-alkyl lipids such as fatty acids and alkanes can be used to discern between marine and terrigenous inputs. For instance, *n*-alkanes and *n*-alkanoic acids (also known as fatty acids) in terrigenous plants consist of a high number of carbon atoms (number of carbon atoms  $\geq 24$ ), referred to as high-molecular-weight (HMW) lipids (Eglinton and Hamilton, 1967), and have often been used to elucidate specific sources of terrigenous OM given their resistance to degradation (e.g., Bröder et al., 2018; Wei et al., 2024; Yedema et al., 2023). In contrast, microorganisms such as phytoplankton tend to have shorter-chained alkanes and fatty acids ( $C < 20$ ), often referred to as low-molecular-weight (LMW) lipids (Killops and Killops, 2004). Given the higher reactivity of these latter compounds, it is generally assumed that any detectable LMW lipids mainly represent *in-situ* marine production. In addition, proxies based on *n*-alkyl lipid distributions such as the carbon preference index (CPI; Bray and Evans, 1961) – the ratio of odd and even HMW alkanes or fatty acids – can be used to determine the degree of degradation, with higher CPI for fresher plant waxes, and lower CPI nearing 1 for more degraded compounds (Bray and Evans, 1961; Eglinton and Hamilton, 1967). Finally, compound-specific stable carbon isotope analysis of biomarkers also provides insights into the origin of specific lipids, including sources of terrigenous OM deposited in marine sediments (Tolosa et al., 2013; Tao et al., 2016; Gibbs et al., 2020).

The application of biomarkers to trace the sources of OM in submarine canyons is limited to the use of specific biomarkers such as lignin phenols (Tesi et al., 2008; Pasqual et al., 2013; Paradis et al., 2022), lipid biomarkers (Salvadó et al., 2017; Pruski et al., 2022), or compound-specific stable carbon isotope analyses (Gibbs et al., 2020). In this study, we use multiple sedimentological and geochemical parameters to investigate the quantity, composition, and sources of OC and its dispersal in the submarine canyon system from the Gulf of Palermo, where contrasting canyon characteristics allow assessment of the influence of sediment dispersal mechanisms on the distribution of terrigenous OC along and across this continental margin.

## 2 Methods

### 2.1 Study area

The Gulf of Palermo (Fig. 1), spanning an area of 250 km<sup>2</sup>, lies on the north-western Sicilian margin, bordered by Cape Gallo to the West and Cape Zafferano to the East, two promontories that harbour natural parks characteristic of

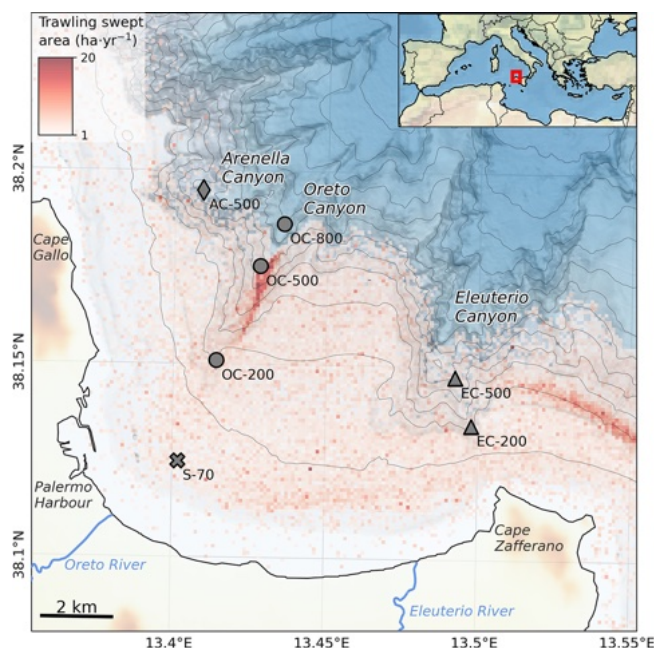


**Figure 1.** Bathymetric map of the Gulf of Palermo, with the three main submarine canyons incising the continental margin (Arenella, Oreto and Eleuterio canyons) as well as the locations of sampled sediment cores, with different symbols based on their geomorphological location (Shelf: cross, Arenella Canyon: diamond, Oreto Canyon: circles, Eleuterio Canyon: triangles). Mean annual trawling intensity is given as swept area per year ( $\text{ha yr}^{-1}$ ) between 2008 and 2016. The dashed line shows the direction of the regional current and contour lines are displayed every 100 m. Adapted from Paradis et al. (2021).

Mediterranean vegetation, including  $C_3$  and  $C_4$  plants (Domina et al., 2025). The circulation pattern on the northern Sicilian shelf is governed by the west-to-east flow of the Modified Atlantic Water (MAW) along the shelf (Istituto Idrografico della Marina, 1982; Pinardi and Masetti, 2000; Arjona-Camas et al., 2024). This regional cyclonic geostrophic current results in a gradual west-east decrease in coastal sediment grain size along the margin, which is interrupted by the presence of the Oreto and Eleuterio rivers that deposit coarser sediment at their river mouths (Tranchina et al., 2008). These two torrential rivers have an average discharge of  $0.25 \text{ m}^3 \text{ s}^{-1}$  that can increase to  $5.3 \text{ m}^3 \text{ s}^{-1}$ , in the case of Eleuterio River, and  $26.3 \text{ m}^3 \text{ s}^{-1}$ , in the case of Oreto River, during flood events (Mannina and Viviani, 2010; Billi and Fazzini, 2017). The Gulf of Palermo is highly polluted, primarily due to urban and harbour operations.

The Gulf of Palermo is incised by several submarine canyons. The most prominent are the Arenella, Eleuterio, and Oreto canyons, which are important conduits for the dispersal of sediment (Lo Iacono et al., 2011, 2014; Paradis et al., 2021). In the northwestern sector of the Gulf lies the smallest of these canyons, Arenella Canyon, which incises the steep

continental slope and the shelf edge. The Oreto Canyon incises the slope and the outer shelf on the central sector of the gulf, and although it developed in connection with the Oreto River during low stands of sea-level (Lo Iacono et al., 2011), it is presently not directly connected to this river, currently being separated by a 5 km-wide shelf. Despite the close proximity of Eleuterio Canyon to the Eleuterio River, there is no evidence that they were connected during the last sea-level low stand (Lo Iacono et al., 2014). Instead, the canyon's axial incision at its head, oriented towards Cape Zafferano, shortens the width of the shelf and reduces the distance from the shoreline to approximately 2 km. This configuration facilitates the transport of suspended sediment from the shelf into Eleuterio Canyon, leading to naturally high sedimentation rates ( $0.52 \text{ cm yr}^{-1}$ ) along its axis at 200 m in comparison to natural sedimentation rates in Oreto Canyon at the same depth ( $0.11\text{--}0.16 \text{ cm yr}^{-1}$ ) (Paradis et al., 2021).

Besides natural sediment transport processes, bottom trawling activities in the Gulf of Palermo have been occurring on the continental shelf and upper slope, as well as along Oreto Canyon since the 1970–1980s (Fig. 1; Paradis et al., 2021). The continuous contact of demersal fishing gear with the seafloor has contributed to sediment resuspension and its posterior transfer into these three submarine canyons, causing sedimentation rates to increase by up to an order of magnitude ( $0.73\text{--}1.38 \text{ cm yr}^{-1}$ ) in comparison to natural (i.e., pre-1980s) background sedimentation ( $0.11\text{--}0.16 \text{ cm yr}^{-1}$ ) (Paradis et al., 2021; Arjona-Camas et al., 2024). This alteration in sedimentary dynamics contributed to the dilution of OC in these submarine canyons caused by the transfer of older and coarser sediment, with lower concentrations of contaminants (Palanques et al., 2022).

## 2.2 Sampling

Seven sediment multicores were collected in the Gulf of Palermo in the framework of the FP7 EU-Eurofleets2 ISLAND (Exploring Sicilian Canyon Dynamics) cruise on board the R/V *Angeles Alvariño* on August 2016. One sediment multicore was collected on the shelf at 70 m water depth (S-70),  $\sim 2.5$  km off the Oreto River mouth and the Palermo harbour (Fig. 1). The other six multicores were collected within the three studied submarine canyons: one in Arenella Canyon at 500 m depth (AC-500), three along the Oreto Canyon at 200, 500 and 800 m depth (OC-200, OC-500, OC-800), and two along the Eleuterio Canyon at 200 and 500 m depth (EC-200, EC-500) (Fig. 1).

Sediment cores were collected using a K/C Denmark six-tube multicorer (inner diameter 9.4 cm), and the core with the best-preserved sediment-water interphase was subsampled at 1 cm intervals and stored in sealed plastic bags at  $-20^\circ\text{C}$  until freeze-dried in the laboratory for analysis. In addition, triplicate sediment cores were collected at 500 m depth of all canyons (AC-500, OC-500, EC-500) for the analyses of the OM composition (total lipids, proteins, carbohydrates, and

phytopigments). Only surficial sediment sections (0–1 cm) were used for the present study. A full description of the sediment core sampling strategy is given in Table S1.

## 2.3 Sedimentary characteristics

Grain size distributions were determined using a Horiba Partica LA950V2 particle size analyser following oxidation of 1–4 g of dried sediment using 20 %  $\text{H}_2\text{O}_2$  and disaggregation using 2.5 %  $\text{P}_2\text{O}_7^{4-}$ . Down-core data of sediment grain size distributions were described and published by Paradis et al. (2021) and Palanques et al. (2022).

To complement grain size analyses, mineral surface area was measured on sediment samples that were slow-heated at  $350^\circ\text{C}$  for 12 h to remove OM, using a 5-point BET (Brunauer-Emmett-Teller adsorption isotherm, Brunauer et al., 1938) method on a NOVA 4000 surface area analyser (Quantachrome Instrument). Prior to analysis, samples were degassed with a Quantachrome FLOVAC degasser at  $350^\circ\text{C}$  for 2 h.

## 2.4 Elemental analysis and isotopic composition

Organic carbon (OC) and total nitrogen (TN) contents were measured using a Thermo EA 1108 elemental analyser (EA) at the Scientific-Technical Services of the University of Barcelona. Samples for OC analysis were first decarbonated using repeated additions of  $100 \mu\text{L}$  25 % HCl with  $60^\circ\text{C}$  drying steps in between until no effervescence occurred. Down-core data of OC and TN were described and presented in detail by Palanques et al. (2022).

Stable carbon isotopic composition ( $\delta^{13}\text{C}$  values) was determined on  $200 \mu\text{g}$  of OC after fumigating the samples in a desiccator at  $60^\circ\text{C}$  in silver capsules with concentrated HCl (37 %) during 72 h to remove all inorganic carbon, neutralized under basic atmosphere using NaOH pellets for another 72 h, and subsequently wrapped in tin capsules. Samples were analysed on an EA coupled in continuous flow with an Isoprime PrecisION stable isotope ratio mass spectrometer (EA-iRMS). Values are reported relative to the Vienna Pee Dee Belemnite reference material and precision was  $0.19\text{‰}$  ( $1\sigma$ ) based on replicate measurements of standards. For  $\delta^{15}\text{N}$  measurements, approximately 50 mg of non-decarbonated sediment was analysed on the same EA-iRMS, with  $\delta^{15}\text{N}$  values reported relative to  $\text{N}_2$  in the air. Samples were calibrated against atropine (Säntis, PN – SA990746B, LN – 51112) and Pepton Sigma (PN = P7750-100G, LN = SLBC5290V) which were used as standards.

A separate subsample was fumigated following the same procedure and radiocarbon content was measured in a Mini Carbon Dating System (MICADAS) with a gas ion source at the Laboratory of Ion Beam Physics, ETH Zürich, and reported as conventional radiocarbon age and  $\Delta^{14}\text{C}$  (Stuiver and Polach, 1977). Samples were calibrated against oxalic acid II (NIST SRM 4990C) and phthalic anhydride (Sigma,

PN-320064-500g, LN-MKBH1376V) which were used as standards for these analyses.

## 2.5 Biochemical composition of sedimentary organic matter

Total proteins, carbohydrates, and lipids were quantified spectrophotometrically using a Varian Cary 50UV-Vis following the methods described by Hartree (1972) and modified by Rice (1982), Gerchakov and Hatcher (1972), and Bligh and Dyer (1959), and Marsh and Weinstein (1966), respectively. The analysis of proteins and lipids was performed on 0.1–0.6 g of frozen sediment (0.05–0.3 g of dry sediment), whereas carbohydrate analysis was performed on ~0.1 g of previously dried sediment. Protein, carbohydrate, and lipid contents were normalized to OC content and expressed as  $\text{mgC g}^{-1}$  OC after conversion to carbon equivalents using the factors  $0.49 \text{ mgC g}^{-1}$  for proteins,  $0.40 \text{ mgC g}^{-1}$  for carbohydrates, and  $0.75 \text{ mgC g}^{-1}$  for lipids (Fabiano et al., 1995). Chlorophyll *a* and phaeopigments, after acidification of wet sediment with 0.1 N HCl, were extracted using acetone 90 % overnight, in the dark at 4 °C and quantified fluorometrically (Shimadzu RF-6000) according to Lorenzen and Jeffrey (1980) and modified by Danovaro (2009) for sediments. Total phytopigment concentrations were defined as the sum of chlorophyll *a* and phaeopigment concentrations and converted into carbon equivalents using a conversion factor of 40 (Pusceddu et al., 2010).

Organic matter reactivity was assessed by calculating the protein turnover rates, as N is considered to be the primary limiting factor for heterotrophic nutrition and proteins are rich in nitrogen. Protein turnover rates were derived from measurements of extracellular aminopeptidase activity. This activity was determined using a fluorometric method, where about 0.1 g of sediment was incubated for one hour in the dark with  $100 \mu\text{M}$  of the substrate L-leucine-4-methylcumarinyl-7-amide. When cleaved by aminopeptidase enzymes, this substrate emits fluorescence, with the intensity reflecting the level of enzyme activity (in terms of degraded substrate per g of sediment per hour). Fluorescence was measured both before and after incubation, and the difference was used to estimate the amount of degraded substrate (proxy for the enzyme activity; Danovaro, 2009). The resulting values were converted into carbon units using a conversion factor of  $72 \text{ ng C per nmol of substrate}$  (Fabiano and Danovaro, 1998). Protein turnover rates were then determined by dividing the protein-derived carbon degradation rates by the total protein-carbon content in the sediment. Due to limited sample availability, these analyses were only performed in selected samples.

Lipids were further extracted and separated into GDGTs and fatty acids. Briefly, total lipids were extracted from ~0.5 g dried sediment samples in dichloromethane (DCM):methanol 9 : 1 (*v/v*) using an energized dispersive guided extraction (CEM EDGE) system. The resulting ex-

tracts were dried under nitrogen flow and saponified with 0.5M KOH solution in methanol for 2 h at 70 °C. The neutral and acid fractions were separated using solvent-solvent extraction with hexane. The neutral (hexane) fraction was further separated into an apolar fraction and a polar fraction (including GDGTs) using a deactivated (1 %) silica column with a solvent mixture of hexane : DCM 9 : 1 and DCM : methanol 1 : 1, respectively. An internal  $\text{C}_{46}$  GDGT standard (Huguet et al., 2006) was added to the polar fraction to determine GDGT concentrations and the fraction was filtered on a  $0.45 \mu\text{m}$  PTFE syringe filter. GDGTs were measured on an Agilent 1260 infinity series LC-MS following the methods described by Hopmans et al. (2016). We calculate the Branched and Isoprenoid Tetraether (BIT) index (Hopmans et al., 2004), which takes the ratio of brGDGTs and isoGDGTs to help identify the relative contribution of terrigenous-derived OM and marine-produced OM, assuming that brGDGTs are exclusively of terrigenous origin, and isoGDGTs are exclusively of marine origin. This proxy was calculated as follows, employing the roman numerals for each GDGT molecule as denoted by Sinninghe Damsté (2016):

$$\text{BIT} = \frac{[(\text{Ia}) + (\text{IIa}) + (\text{IIIa}) + (\text{IIa}') + (\text{IIIa}')] }{[(\text{Ia}) + (\text{IIa}) + (\text{IIIa}) + (\text{IIa}') + (\text{IIIa}') + (\text{IV})]} \quad (1)$$

Fatty acids were extracted from the acid fraction after acidification to pH 2 using hexane : DCM 4 : 1, and were subsequently derivatized into corresponding fatty acid methyl esters (FAMES) with MeOH : HCl (95 : 5, 12 h at 70 °C). FAMES were quantified on a GC-FID (gas chromatograph connected to a flame ionization detector, Agilent 7890A). The temperature program started with a 1 min hold time at 50 °C, followed by a  $10 \text{ }^\circ\text{C min}^{-1}$  ramp to 320 °C and a 5 min hold time at 320 °C. Peaks were identified against a mixture of pure standard compounds based on retention time.

The carbon preference index (CPI; Bray and Evans, 1961) was calculated for the high molecular weight fatty acids as follows:

$$\text{CPI}_{(\text{C}_{24}-\text{C}_{32})} = \frac{1}{2} \cdot \frac{\sum (\text{C}_{24} - \text{C}_{30})_{\text{even}} + \sum (\text{C}_{26} - \text{C}_{32})_{\text{even}}}{\sum (\text{C}_{25} - \text{C}_{29})_{\text{odd}}} \quad (2)$$

Isotopic ( $\delta^{13}\text{C}$ ) analyses were further conducted on isolated FAME fractions in duplicate by GC-isotope ratio mass spectrometry (GC-IRMS) on a Thermo Trace GC (1310) coupled with a Thermo Delta-V plus system. The GC was equipped with an RTX-200 MS capillary column ( $60 \text{ m} \times 0.25 \text{ mm i.d.}$ ,  $0.25 \mu\text{m}$  film thickness) that was programmed to first heat up to 120 °C at  $40 \text{ }^\circ\text{C min}^{-1}$  and then ramp to 320 °C at  $6 \text{ }^\circ\text{C min}^{-1}$ , with a hold time at 320 °C for 12 min. An external standard with known  $\delta^{13}\text{C}$  value (Mix A7 Arndt Schimmelmann, Indiana University, USA) was run every 10 samples to assess the drift of the instruments. The  $\delta^{13}\text{C}$  values of the fatty acids were corrected for the additional C from methylation ( $\delta^{13}\text{C}_{\text{C-MeOH}} =$

$-48.09 \pm 0.41$  ‰), and accounting for the number of carbon atoms ( $n$ ) of each FAME as follows:

$$\delta^{13}\text{C}_{\text{FA}} = \frac{(n_{\text{CFA}} + 1) \cdot \delta^{13}\text{C}_{\text{FAME measured}} - 1 \cdot \delta^{13}\text{C}_{\text{C-MeOH}}}{n_{\text{CFA}}} \quad (3)$$

Since  $\delta^{13}\text{C}$  of the FAME fractions could only be measured on specific carbon chains ( $\text{C}_{16}$ – $\text{C}_{28}$ ), weighted-average  $\delta^{13}\text{C}$  values of HMW FA were calculated as follows:

$$\delta^{13}\text{C}_{\text{HMW FA}} = \frac{\sum(\delta^{13}\text{C}_{24-28} \cdot \text{C}_{24-28})}{\sum(\text{C}_{24} - \text{C}_{28})} \quad (4)$$

## 2.6 Mixing models

To estimate the proportional contributions of terrigenous and marine OC deposited in the Gulf of Palermo submarine canyon system, we employed a Bayesian isotope mixing model that utilizes Markov Chain Monte Carlo (MCMC) methods to estimate posterior distributions of source contributions following (Andersson, 2011) and adapting the MixSIAR model (Stock et al., 2018) to Python's PyMC library (Abril-Pla et al., 2023).

We estimated the contribution of terrigenous and marine OC using several approaches. We applied a one-dimensional mixing model employing only  $\delta^{13}\text{C}$  values as endmembers of marine and terrigenous OC. We then applied a two-dimensional mixing model combining  $\delta^{13}\text{C}$  with OC/TN,  $\delta^{15}\text{N}$ , and  $\Delta^{14}\text{C}$ , respectively (see Table 1 for postulated end-member value ranges from published literature).

In the different one-dimensional and two-dimensional mixing models, each model was run 4000 times using MCMC sampling of the ranges of endmember values, assuming they follow a normal distribution. Posterior distributions of source proportions were summarized using the mean and the highest density interval at 68 %, representative of one standard deviation.

## 3 Results

### 3.1 Sedimentological, elemental and isotopic composition

Median grain size of surficial sediment from the Gulf of Palermo and its submarine canyons system did not exhibit a clear offshore trend, mostly ranging between 23  $\mu\text{m}$  and 25  $\mu\text{m}$ , with the exception of the Oreto canyon head (OC-200) at 13  $\mu\text{m}$  and the Eleuterio mid-canyon (EC-500) at 10  $\mu\text{m}$  (Fig. S1). Similarly, mineral surface area did not present any clear spatial pattern, with values generally ranging between 11 and 15  $\text{m}^2 \text{g}^{-1}$ , with the exception of the Eleuterio mid-canyon (EC-500) at 21  $\text{m}^2 \text{g}^{-1}$  which had the largest mineral surface area in agreement with the finest median grain size, given the close relationship between these two parameters (Fig. S1).

The spatial distribution of surface OC in this system exhibited a slight offshore decrease from 1.6 % on the shelf (S-70) to  $\sim 1.2$  % inside the canyons, with lowest OC contents (1.1 %) in Oreto mid-canyon (OC-500) (Fig. 2a). TN content presented a similar offshore trend, although highest values (0.17 %) were observed in the Oreto canyon head (OC-200), and lowest values (0.13 %) in both Oreto mid-canyon (OC-500) and Arenella mid-canyon (AC-500) sites (Fig. S2a). The OC/TN molar ratio presented a modest offshore decrease from 9 at S-70 to 8 in Arenella mid-canyon (AC-500) and to values of  $\sim 6$  inside Oreto and Eleuterio canyons (Fig. 2b). Given the spatial distribution of grain size and mineral surface area across this canyon system, OC contents were normalized to mineral surface area (OC/SA) to assess the distribution of “OC loading” to account for the influence of hydrodynamic sorting of fine-grained sediment that is enriched in OC as well as its transformation during its transport. OC loading exhibited a clear offshore decrease across the gulf from 1.3  $\text{g m}^{-2}$  in S-70 to 0.6  $\text{g m}^{-2}$  in EC-500, presumably reflecting OC degradation during transit (Fig. 2c).

The spatial distribution of  $\delta^{13}\text{C}$  values of bulk OC presented a general offshore increase, ranging from  $-27$  ‰ on the shelf (S-70) to  $-21$  ‰ in Arenella mid-canyon (AC-500) (Fig. 2d). Isotopic composition varied among canyons, with lower values in Eleuterio Canyon ( $-26$  ‰ to  $-23$  ‰), in comparison to Oreto Canyon ( $-24$  ‰ to  $-21$  ‰) and Arenella Canyon ( $-21$  ‰). The spatial distribution of  $\delta^{15}\text{N}$  values of surface sediment was relatively invariant, ranging between 6 ‰ to 7.2 ‰ (Fig. 2e). Nevertheless, there was a general offshore increase from 6 ‰ on the shelf (S-70) to 7.2 ‰ in Eleuterio mid-canyon (EC-500) (Fig. 2e).

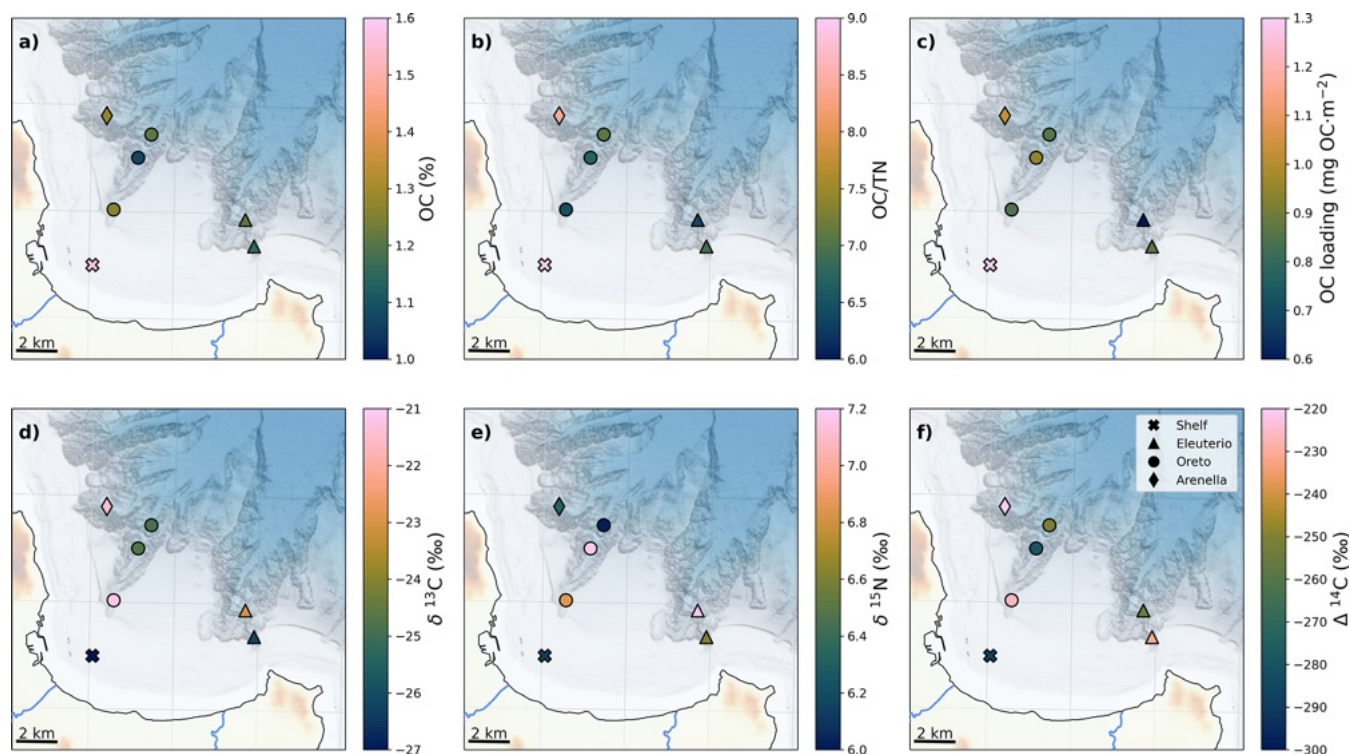
In the case of radiocarbon contents of OC, the sediment core from the shelf (S-70) had the lowest (oldest)  $\Delta^{14}\text{C}$  values of  $-286.4 \pm 0.7$  ‰, equivalent to  $2646 \pm 71$  years before present (yr BP). Within the submarine canyons, there was a general offshore decrease in  $\Delta^{14}\text{C}$ , indicative of down-canyon ageing of OC (Figs. 2f, S2b). Arenella mid-canyon (AC-500) had the highest  $\Delta^{14}\text{C}$  of  $-220.2 \pm 0.8$  ‰, whereas in both Eleuterio and Oreto canyons,  $\Delta^{14}\text{C}$  values decreased from  $-230.5 \pm 0.8$  ‰ and  $-226.6 \pm 0.8$  ‰ at their heads (EC-200 and OC-200, respectively), to  $-253.7 \pm 0.7$  ‰ and  $-250.9 \pm 0.7$  ‰ at Eleuterio mid-canyon (EC-500) and Oreto canyon mouth (OC-800), respectively, corresponding to a  $\sim 250$  years down-canyon ageing of OC. This general down-canyon decrease in  $\Delta^{14}\text{C}$  values was interrupted in Oreto mid-canyon (OC-500), which exhibited the oldest ( $2568 \pm 70$  yr BP) and lowest  $\Delta^{14}\text{C}$  value of  $-286.4 \pm 0.7$  ‰ (Figs. 2f, S2b).

### 3.2 Organic matter composition

The composition of OM in terms of proteins, lipids, and carbohydrates generally varied offshore with different water depth-related patterns in each canyon (Fig. 3a–c). Lowest protein concentrations of  $99 \pm 9 \text{ mgC g}^{-1}$  OC

**Table 1.** Ranges of marine and terrigenous endmembers for  $\delta^{13}\text{C}$ , OC / TN,  $\delta^{15}\text{N}$ , and  $\Delta^{14}\text{C}$ , as well as the location where these values were obtained.

Endmember	Marine	Terrigenous	Locations	References
$\delta^{13}\text{C}$	-21‰ to -19‰	-32‰ to -26‰	Gulf of Lions Sicily soils Catalan rivers	Harmelin-Vivien et al. (2008), Sanchez-Vidal et al. (2013), Lawrence et al. (2020)
OC / TN	5 to 9	8 to 13	Gulf of Lions Catalan rivers	Harmelin-Vivien et al. (2008), Sanchez-Vidal et al. (2013)
$\delta^{15}\text{N}$	4‰ to 16‰	3‰ to 5‰	Gulf of Lions Catalan rivers	Harmelin-Vivien et al. (2008), Sanchez-Vidal et al. (2013)
$\Delta^{14}\text{C}$	0‰ to 100‰	-310‰ to -66‰	Sicily soils	Lawrence et al. (2020)

**Figure 2.** Spatial distribution of bulk parameters: (a) OC, (b) OC / TN, (c) OC loading, (d)  $\delta^{13}\text{C}$ , (e)  $\delta^{15}\text{N}$ , (f)  $\Delta^{14}\text{C}$ . Colour bars are adjusted to highlight the minimum, mean, and maximum values for each variable.

were observed in Arenella mid-canyon (AC-500) (Fig. 3a). In contrast, highest protein concentrations were observed in Oreto Canyon, where concentrations decreased down-canyon from  $222 \pm 2 \text{ mgC g}^{-1}$  OC at its head (OC-200) to  $109 \pm 10 \text{ mgC g}^{-1}$  OC at its mouth (OC-800), the latter being comparable to concentrations in AC-500. Eleuterio Canyon had slightly lower protein concentrations ( $\sim 200 \text{ mgC g}^{-1}$  OC) than in the other canyons (Fig. 3a). Highest carbohydrates concentrations were detected in Oreto Canyon head (OC-200), where concentrations decreased down-canyon from  $311 \pm 32 \text{ mgC g}^{-1}$  OC to  $247 \pm 21 \text{ mgC g}^{-1}$  OC, with minimum values of

$46 \pm 1 \text{ mgC g}^{-1}$  OC at mid-canyon (OC-500) (Fig. 3b). Carbohydrate concentrations were slightly lower in Eleuterio Canyon, where values decreased down-canyon from  $270 \pm 8 \text{ mgC g}^{-1}$  OC at the canyon head (EC-200) to  $39 \pm 6 \text{ mgC g}^{-1}$  OC at mid-canyon (EC-500), the latter similar to the carbohydrate concentrations observed at the same mid-canyon depths in both Arenella and Oreto canyons (Fig. 3b). Lipid concentrations were highest in Arenella Canyon, with  $111 \pm 2 \text{ mgC g}^{-1}$  OC, and lowest in Oreto Canyon, where values decreased offshore from  $76 \pm 10$  to  $51 \pm 2 \text{ mgC g}^{-1}$  OC. Eleuterio Canyon had intermediate con-

centrations of  $66 \pm 3 \text{ mgC g}^{-1} \text{ OC}$  and  $62 \pm 4 \text{ mgC g}^{-1} \text{ OC}$  in its head and mid-canyon (Fig. 3c).

Concentrations of phytopigments did not present a general offshore decrease and were more variable between canyons (Fig. 3d). Lowest concentrations of  $13 \text{ mgC g}^{-1} \text{ OC}$  were observed both in S-70 and OC-500, whereas highest concentrations were observed in Arenella Canyon ( $17.8 \pm 1.0 \text{ mgC g}^{-1} \text{ OC}$ ) and Eleuterio Canyon (EC-200:  $17.1 \pm 2.1 \text{ mgC g}^{-1} \text{ OC}$ ; EC-500:  $16.6 \pm 0.2 \text{ mgC g}^{-1} \text{ OC}$ ).

Protein turnover rates in selected sediment samples showed a general increase with depth and distance from shore (Fig. S2c). Lowest turnover rates were measured in Eleuterio canyon head (EC-200,  $0.85 \pm 0.20 \text{ yr}^{-1}$ ) which increased with depth (EC-500,  $4.69 \pm 0.99 \text{ yr}^{-1}$ ). In Oreto Canyon, turnover rates also increased downcanyon where highest turnover rates were observed in the canyon mouth (OC-500,  $2.52 \pm 0.54 \text{ yr}^{-1}$ ; OC-800,  $17.5 \pm 1.8 \text{ yr}^{-1}$ ). Finally, Arenella mid-canyon had the highest turnover rates in comparison to the other sediment samples located at a similar depth-range (AC-500,  $12.1 \pm 2.7 \text{ yr}^{-1}$ ).

### 3.3 Lipid biomarkers

Specific sources of OM were assessed based on concentrations and ratios of GDGTs and *n*-alkanoic acid (fatty acid, FA) biomarkers. Unfortunately, during the separation of GDGTs, the extract from Eleuterio mid-canyon (EC-500) was lost and insufficient material was available to re-extract lipids from this sample.

Surficial sediment in all sites presented detectable amounts of branched GDGTs (brGDGTs) and isoprenoid GDGTs (isoGDGTs). Concentrations of isoGDGTs were an order of magnitude higher than brGDGTs, with crenarchaeol as the most abundant isoGDGT ( $51 \pm 2\%$ ) (Fig. S4a, b). Crenarchaeol concentrations exhibited no distinct pattern with depth or distance from shore (Fig. 4a). Crenarchaeol concentrations were highest ( $420 \mu\text{g g}^{-1} \text{ OC}$ ) in the Oreto canyon head (OC-200), where it decreased downcanyon to  $340 \mu\text{g g}^{-1} \text{ OC}$  at mid-canyon (OC-500) with minimum values of  $210 \mu\text{g g}^{-1} \text{ OC}$  detected in the canyon mouth (OC-800) (Fig. 4a). Relatively similar crenarchaeol concentrations of  $\sim 230 \mu\text{g g}^{-1} \text{ OC}$  were detected in the remaining sites. The BIT index did not follow a clear pattern with depth or distance from shore either, and was considerably low across the entire study area (0.025–0.05) (Fig. S3c).

The concentrations of LMW FA ( $C < 20$ ) ranged from 13 to  $35 \mu\text{g g}^{-1} \text{ OC}$ , and the concentrations of HMW FA ( $C \geq 24$ ) ranged from 18 to  $25 \mu\text{g g}^{-1} \text{ OC}$  (Fig. 4b, c). There was no apparent trend with depth for neither LMW nor HMW FA. In the case of LMW FA, concentrations were lowest on the shelf (S-70;  $19 \pm 2 \mu\text{g g}^{-1} \text{ OC}$ ), and slightly higher in Arenella mid-canyon (AC-500;  $25.4 \pm 0.3 \mu\text{g g}^{-1} \text{ OC}$ ). The Oreto canyon head (OC-200) exhibited the highest concentrations of  $35 \pm 3 \mu\text{g g}^{-1} \text{ OC}$  which decreased downcanyon to  $28 \pm 3 \mu\text{g g}^{-1} \text{ OC}$  in the canyon mouth (OC-800),

with minimum concentrations of  $13 \pm 1 \mu\text{g g}^{-1} \text{ OC}$  observed in the mid-canyon site (OC-500). Finally, LMW FA concentrations presented a slight down-canyon increase in Eleuterio Canyon, from  $25.4 \pm 0.3 \mu\text{g g}^{-1} \text{ OC}$  in the canyon head (EC-200) to  $28 \pm 2 \mu\text{g g}^{-1} \text{ OC}$  in the canyon mouth (EC-500) (Fig. 4b).

For the HMW FA, concentrations were highest on the shelf (S-70;  $24.9 \pm 0.1 \mu\text{g g}^{-1} \text{ OC}$ ) and in the mid-canyon site of Arenella Canyon (AC-500;  $25.2 \pm 0.1 \mu\text{g g}^{-1} \text{ OC}$ ). Oreto Canyon presented a slight down-canyon increase from  $21.0 \pm 0.1 \mu\text{g g}^{-1} \text{ OC}$  in the canyon head (OC-200) to  $24.4 \pm 0.1 \mu\text{g g}^{-1} \text{ OC}$  in the canyon mouth (OC-800), with lowest concentrations of  $18.1 \pm 0.1 \mu\text{g g}^{-1} \text{ OC}$  in the mid-canyon (OC-500) (Fig. 4c). The  $\text{CPI}_{(C_{24}-C_{32})}$  had relatively low values and fell within a narrow range between 1.8 and 2.4. Lowest  $\text{CPI}_{(C_{24}-C_{32})}$  were observed in S-70, AC-500 and OC-800 (1.8–1.9), intermediate values ranging between 2.1 and 2.2 were observed in OC-200, OC-500 and EC-200, and highest  $\text{CPI}_{(C_{24}-C_{32})}$  values of 2.4 in EC-500 (Fig. S3f).

Compound-specific  $\delta^{13}\text{C}$  values of individual fatty acid homologues vary from  $-25\%$  to  $-30\%$  (Fig. 5). The  $\delta^{13}\text{C}$  signature decreased from  $-27.6 \pm 0.3\%$  in  $\text{C}_{16}$  to  $-29.9 \pm 0.4\%$  in  $\text{C}_{22}$  fatty acids. For  $\text{C}_{24}$  to  $\text{C}_{28}$  compounds,  $\delta^{13}\text{C}$  values increased to as high as  $-26.1 \pm 0.5\%$  for the samples in Arenella and Oreto canyons, whereas the increase of  $\delta^{13}\text{C}$  was more modest for the shelf and Eleuterio Canyon, reaching  $-28.7 \pm 0.4\%$ . The concentration-weighted average  $\delta^{13}\text{C}$  signature of HMW FA showed a distinct spatial variation across canyons (Fig. 4d). Higher  $\delta^{13}\text{C}$  values of  $-26.3 \pm 0.3\%$  were observed in the Arenella Canyon, which decreased to  $-27.4 \pm 0.2\%$  in the Oreto Canyon, and further decreased to  $-29.2 \pm 0.5\%$  in the Eleuterio Canyon, which was similar to the shelf site (Fig. 4d).

### 3.4 Source allocation through mixing models

Considering the range of values of terrigenous and marine end-members, there is a general shift of  $\delta^{13}\text{C}$  composition from more terrigenous to more marine values with depth (Fig. S4). However, when combining the  $\delta^{13}\text{C}$  values with OC/TN and  $\delta^{15}\text{N}$ , the trend is not that clear. Nevertheless, the fraction of terrigenous OC provided by the Bayesian Markov-Chain Monte-Carlo mixing model in one dimension with only  $\delta^{13}\text{C}$ , as well as in two-dimensional mixing models of  $\delta^{13}\text{C}$  coupled with OC/TN,  $\delta^{15}\text{N}$ , or  $\Delta^{14}\text{C}$  showed a general offshore decrease from 80% to 20%–40%, depending on the model (Fig. S5).

The spatial variations of the source apportionment were very similar between the one-dimensional mixing model and the two-dimensional mixing model with OC/TN and  $\delta^{15}\text{N}$ , although these models provided highest uncertainties (Fig. S5). In these three models, the offshore decrease of the terrigenous OC fraction was interrupted by a sudden drop in Oreto Canyon at 200 m (OC-200), which presented minimum terrigenous fraction (15%–19%). This low terrigenous

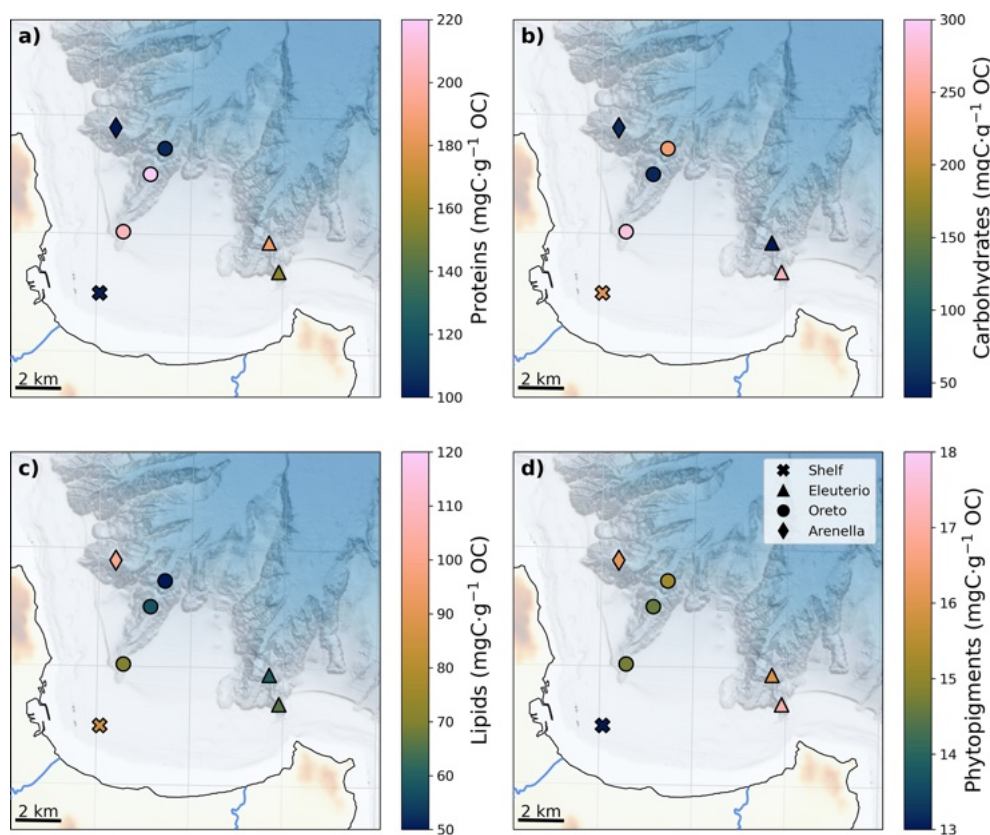


**Figure 3.** Spatial distribution of composition of organic matter: (a) proteins, (b) carbohydrates, (c) lipids, and phytopigments. Colour bars are adjusted to highlight the minimum, mean, and maximum values for each variable.

fraction presents a stark contrast to the terrigenous OC fractions (48 %–60 %) in sediment cores collected further down-canyon at 500 m (OC-500) and 800 m (OC-800). The sediment core collected in Arenella Canyon (AC-500) also presented a similarly low terrigenous OC fraction of 20 %.

In the dual end-member mixing model with  $\delta^{13}\text{C}$  and  $\Delta^{14}\text{C}$  (Fig. S5), both OC-200 and AC-500 also presented the lowest terrigenous fraction, but only of 47 %–55 % in comparison to the lowest terrigenous OC fraction of 15 %–19 % presented by the other models.

## 4 Discussion

### 4.1 Contribution of terrigenous and marine organic carbon in the Gulf of Palermo

The contribution of terrigenous and marine OC deposited in the Gulf of Palermo and its submarine canyons system was assessed by combining an array of bulk parameters (e.g.,  $\delta^{13}\text{C}$ ,  $\Delta^{14}\text{C}$ ,  $\delta^{15}\text{N}$ , OC/TN). While  $\delta^{13}\text{C}$  is the most used proxy for OC source apportionment in one-dimensional mixing models (Pedrosa-Pàmies et al., 2013; Wei et al., 2024), if both  $\text{C}_3$  and  $\text{C}_4$  plants are present in the terrigenous ecosystem, as is the case in the Gulf of Palermo (Domina et al.,

2025),  $\delta^{13}\text{C}$  values of terrigenous and marine OC sources can overlap, hindering source apportionment (Goñi et al., 1998; Gordon and Goñi, 2003). It is important to note that, while the  $\delta^{13}\text{C}$  signatures of terrigenous and marine endmembers adopted for our study area are quite distinct and do not overlap, they were not obtained directly in the Gulf of Palermo region, but rather from similar Mediterranean environments (Table 1). Hence, we further constrain the proportion of terrigenous and marine OC using dual end-member models, which provide an additional dimension and restriction to the calculations for source allocation (Fig. S4).

The application of mixing models using different proxies relies on the assumption that their signatures are conservative and are thus not modified by degradation processes, but this is rarely the case. Even  $\delta^{13}\text{C}$  values are subject to change given that they reflect a composite signature of individual compounds that make up the OC. Preferential degradation of specific compounds can shift the  $\delta^{13}\text{C}$  signature of residual OC (Komada et al., 2012; Lalonde et al., 2014). However, the most important caveats in the aforementioned proxies are associated with OC/TN ratios, as well as  $\delta^{15}\text{N}$ , and  $\Delta^{14}\text{C}$  values, since they experience the greatest alterations through degradation without necessarily reflecting a change in the proportions of terrigenous and marine OC (Meyers,

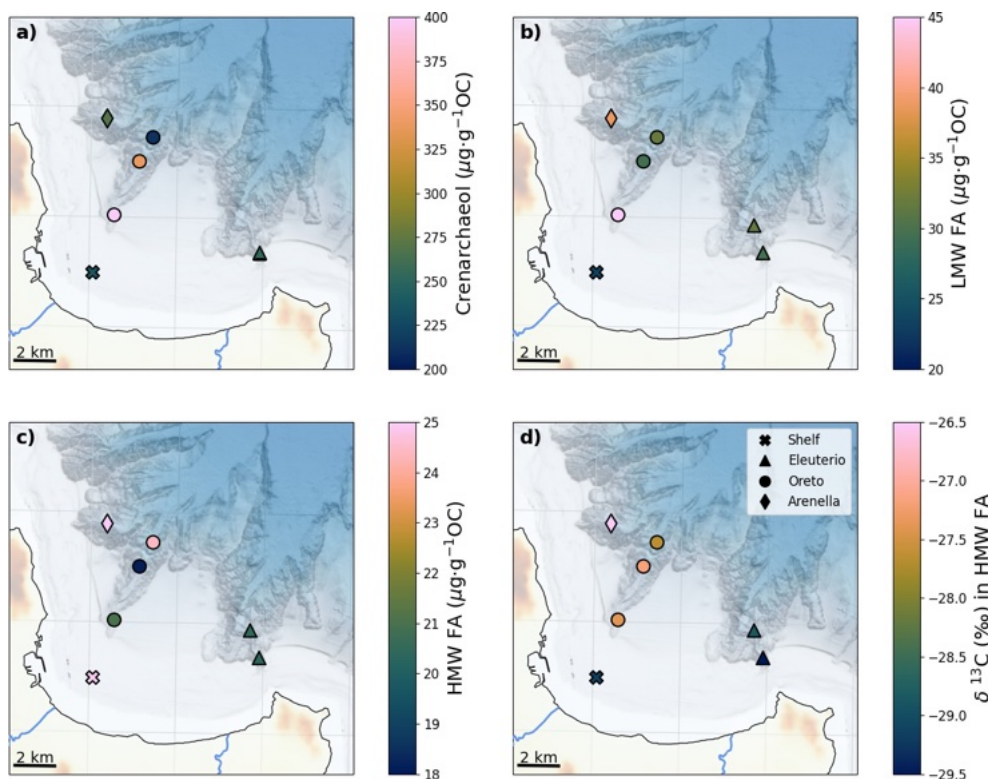


**Figure 4.** Spatial distribution of concentrations of (a) crenarchaeol, (b) LMW FA ( $\text{C}_{16}\text{--}\text{C}_{18}$ )<sub>even</sub>, (c) HMW FA ( $\text{C}_{24}\text{--}\text{C}_{32}$ )<sub>even</sub>, and (d) spatial distribution of  $\delta^{13}\text{C}$  signature of HMW FA ( $\text{C} \geq 24$ ). Colour bars are adjusted to highlight the minimum, mean, and maximum values for each variable.

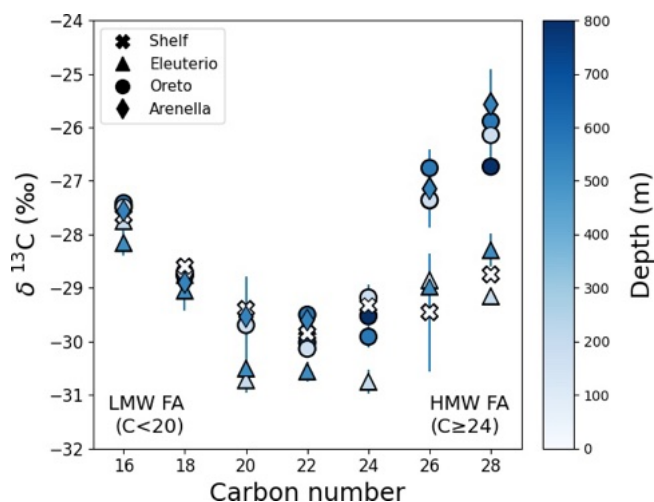


**Figure 5.** Compound-specific  $\delta^{13}\text{C}$  signature of each fatty acid compound.

1994; Lehmann et al., 2002; Komada et al., 2012; Briggs et al., 2013). Hence, we employ biomarkers to further evaluate the use and limitations of these proxies.

OM of terrigenous origin tends to have a higher OC / TN ratio than marine OM, but the preferential degradation of N-

containing components (e.g., proteins) can also modify this ratio, hindering the use of this proxy to determine the sources of OM (Meyers, 1994; Briggs et al., 2013). We deduce that the spatial variation in OC / TN is mostly influenced by degradation rather than source since, for instance, Arenella mid-canyon (AC-500) had one of the highest  $\delta^{13}\text{C}$  values ( $-22\text{‰}$ ), similar to marine endmember, but its OC / TN ratio (8.4) was also one of the highest in the study area, within the values of terrigenous endmember (Fig. S4a). Hence, OC / TN is not an adequate proxy to constrain sources of OC deposited in the Gulf of Palermo. In the case of  $\delta^{15}\text{N}$ , there is no pattern in its signature in relation to  $\delta^{13}\text{C}$  (Fig. S4b), possibly due to the diverse inputs that may contribute to  $\delta^{15}\text{N}$  signatures which complicate its application in source apportionment (Rumolo et al., 2011; Wang et al., 2021), especially considering that this margin is also influenced by anthropogenic pollution (Di Leonardo et al., 2009; Palanques et al., 2022). Finally, while  $\Delta^{14}\text{C}$  values have often been used to constrain the sources of marine and terrigenous OC (Kao et al., 2014; Kim et al., 2022), it can also be modified by degradation (Blair and Aller, 2012; Komada et al., 2012; Bao et al., 2018). In the Gulf of Palermo, the  $\Delta^{14}\text{C}$  signature appears to be mostly driven by source, given the close relationship between  $\Delta^{14}\text{C}$  and phytopigments, where high  $\Delta^{14}\text{C}$  values are indicative of young OC is positively correlated with phy-

topigment concentrations (Fig. S4). Hence, we assume that the  $\delta^{13}\text{C}$ - $\Delta^{14}\text{C}$  mixing model is most appropriate for constraining sources of terrigenous and marine OC in the Gulf of Palermo.

The fraction of terrigenous OC provided by the Bayesian Markov-Chain Monte-Carlo  $\delta^{13}\text{C}$ - $\Delta^{14}\text{C}$  mixing model showed a general offshore decrease from 80 % to 50 % (Fig. 6). The highest fractions of terrigenous OC were observed on the shelf (S-70: 63 %–87 %, for the lower and upper 68 % highest density interval, respectively, see Sect. 2.6), located only 2.5 km from the Oreto River mouth, while minimum terrigenous OC contributions were observed in Arenella mid-canyon (AC-500: 47 %–56 %) as this submarine canyon is located farther north and up-current from both Oreto and Eleuterio rivers. The offshore decreasing trend in terrigenous OC contributions was not apparent for the Oreto Canyon, where minimum terrigenous contributions (47 %–55 %) occurred at the canyon head (OC-200), in comparison to higher terrigenous contributions in the mid-canyon (OC-500: 58 %–73 %) and canyon mouth (OC-800: 53 %–68 %) (Fig. 6). This is counter to the general premise that the contribution of terrigenous OC decreases down-canyon, as observed in other submarine canyons (Pasqual et al., 2013; Pedrosa-Pàmies et al., 2013; Gibbs et al., 2020; Pruski et al., 2022), suggesting more complex dispersal patterns of terrigenous OC (see Sect. 4.3). Finally, Eleuterio Canyon located down-current in the Gulf had decreasing terrigenous OC contribution with depth (EC-200: 54 %–78 %; EC-500: 55 %–63 %). Interestingly, the spatial distribution of OC sources is somewhat related to its reactivity, estimated as protein turnover rates (e.g., Soru et al., 2022, 2024). Highest protein turnover rates were observed in Arenella mid-canyon (AC-500), which had one of the highest marine OC fractions, whereas lowest protein turnover rates were observed in Eleuterio canyon head (EC-200), which had one of the highest terrigenous OC fractions (Fig. S2c). However, we pinpoint here that other factors may also be contributing to the reactivity of OC (see Sect. 4.3).

The fraction of terrestrial OC reaching the submarine canyons in the Gulf of Palermo (50 %–70 %) is considerably lower than in river-connected submarine canyons such as Gaoping Canyon (90 %; Hsu et al., 2014) and Congo Canyon (100 %; Baker et al., 2024). However, this fraction is similar to other non-river connected submarine canyons incising continental shelves such as Hokitika and Kaikoura canyons (70 %–90 % and 50 %, respectively; Gibbs et al., 2020), and higher than in other canyons such as Aviles Canyon (40 %; Romero-Romero et al., 2016), Blanes Canyon (40 %; Pedrosa-Pàmies et al., 2013), and Baltimore Canyon (40 %; Prouty et al., 2017). We acknowledge, though, that the fraction of terrigenous and marine OC deposited in continental margins also depends on marine primary productivity and the consequent flux of marine OC to the seafloor which is lower in Mediterranean margins in comparison to other continental margins: this leads to the accumulation of lower

OC contents in several Mediterranean continental margins in comparison to submarine canyons incising other margins (Pusceddu et al., 2010; Pasqual et al., 2011).

When combined with mass accumulation rates from this area (Paradis et al., 2021), the spatial distribution of marine and terrigenous OC mass accumulation rates can be estimated (Fig. 7). Interestingly, despite the high terrigenous OC content of S-70, this site had the lowest terrigenous OC accumulation rate due to its low sedimentation rate, whereas highest terrigenous accumulation rates occurred in the Eleuterio mid-canyon (EC-500), given the high mass accumulation rate at that site ( $0.82 \text{ g cm}^{-2} \text{ yr}^{-1}$ ; Paradis et al., 2021). In contrast, highest marine OC accumulation occurred in Arenella mid-canyon (AC-500) and in Oreto canyon head (OC-200). Although no data of mass accumulation rate is available from the continental slope, the rapidly decreasing accumulation rates on the shelf with distance from shore ( $0.84$  to  $0.15 \text{ g cm}^{-2} \text{ yr}^{-1}$ ) to values that are considerably lower than in submarine canyons ( $0.35$ – $0.82 \text{ g cm}^{-2} \text{ yr}^{-1}$ ) indicates that sedimentation rates on the adjacent slope will be considerably lower than in the canyon axis, as observed in other incised continental margins (Buscail et al., 1997; Sanchez-Cabeza et al., 1999; Masson et al., 2010; Paradis et al., 2018). Moreover, surficial sediment from a sediment core collected in the open slope between Oreto and Eleuterio canyons at 712 m depth (Di Leonardo et al., 2009) did not present any sign of trace metal contamination, whereas sediment cores collected along the canyon axis had significant trace metal contents, indicating a preferential downslope transfer of sediment and pollutants into submarine canyons (Palanques et al., 2022). In fact, this same sediment core on the slope also presented higher  $\delta^{13}\text{C}$  values ( $-22.7\text{‰}$ ; Di Leonardo et al., 2009), similar to marine end-member values, than those in the afore-mentioned canyons ( $-24\text{‰}$  to  $-25\text{‰}$ ), which tend toward more terrigenous end-member values. This further supports the notion that submarine canyons transfer terrigenous OC deeper and farther offshore than would occur in their absence.

The observed high accumulation of both marine and terrigenous OC in these submarine canyons confirms their role as important sites of OC sequestration, as shown in other canyon systems (Masson et al., 2010; Maier et al., 2019; Baudin et al., 2020). However, the contrasting accumulation of terrigenous and marine OC in each canyon suggests that even in closely spaced submarine canyons, the main source of the OC can greatly differ.

#### 4.2 Sources of terrigenous and marine organic carbon in the Gulf of Palermo

The highest fraction of marine OC (45 %–53 %) as well as marine OC content ( $0.57 \text{ \% dw}$ – $0.68 \text{ \% dw}$ ) are found in surficial sediment of Arenella mid-canyon (AC-500) and Oreto canyon head (OC-200). These sites had the highest  $\delta^{13}\text{C}$  and  $\Delta^{14}\text{C}$  values, trending towards correspond-

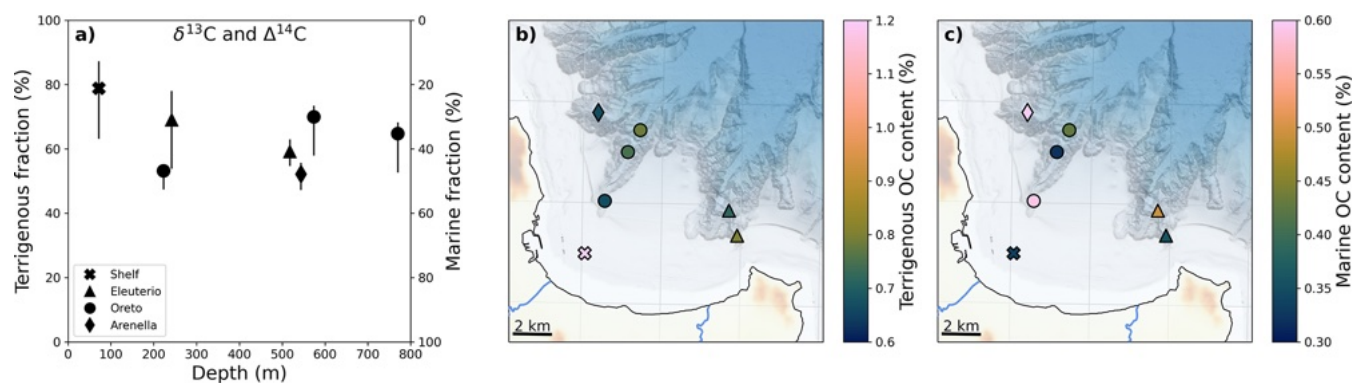


**Figure 6.** Depth and spatial variations in the fraction and content (as a percentage of total sediment) of terrigenous and marine OC obtained from the two-dimensional mixing model based on  $\delta^{13}\text{C}$  and  $\Delta^{14}\text{C}$  values (a–c). Colour bars (b, c) are adjusted to highlight the minimum, mean, and maximum values for each variable.

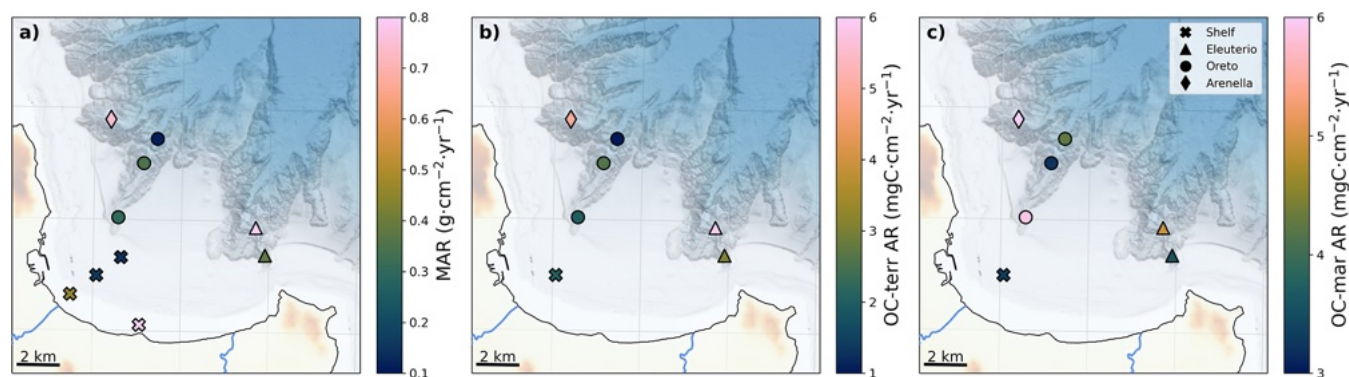


**Figure 7.** Spatial distribution of: (a) mass accumulation rate (MAR) of the studied sediment cores (Paradis et al., 2021) and additional sediment cores from the shelf (Di Leonardo et al., 2007, 2012; Rizzo et al., 2009), (b) terrigenous OC accumulation rate (OC-terr AR), and (c) marine OC accumulation rate (OC-mar AR). Colour bars are adjusted to highlight the minimum, mean, and maximum values for each variable.

ing marine endmembers (Fig. S4c). The high contribution of marine OC in these sites is further confirmed by the biomarker signatures. Phytopigment concentrations were highest in AC-500 ( $17.8 \pm 1.0 \text{ mgC g}^{-1} \text{ OC}$ ) and OC-200 ( $16.0 \pm 1.4 \text{ } \mu\text{gC g}^{-1} \text{ OC}$ ), in comparison to the other sites (Fig. 3d), indicative of high influx of OM from marine phytoplankton. In addition, concentrations of crenarchaeol, an isoGDGT exclusively produced by the ammonia oxidizing archaea Nitrososphaerota commonly found in marine environments (Sinninghe Damsté et al., 2002), were highest in OC-200 ( $400 \text{ } \mu\text{g g}^{-1} \text{ OC}$ ) (Fig. 4a). Interestingly, this site had the highest nitrogen content and nitrogen-rich particulate matter such as proteins (Fig. 3a). Similarly, the concentration of low molecular weight fatty acids (LMW FA), which serves as an indicator of both marine phytoplankton and other (marine) microbial inputs (Volkman et al., 1980; Viso and Marty, 1993; Wakeham and McNichol, 2014), is also highest in OC-200 (Fig. 4b). Altogether, this suggests that, while AC-500 receives primarily marine OM of phytoplankton origin, OC-200 receives marine OM from diverse origins.

Regarding the terrigenous OC distribution, according to the  $\delta^{13}\text{C}$ - $\Delta^{14}\text{C}$  mixing model, the highest proportion of terrigenous OC (0.63–0.87) and terrigenous OC content (1.0%–1.4% dw), occurred on the shelf at 72 m water depth (S-70), only  $\sim 2.5$  km off the Oreto river mouth, and terrigenous OC contributions generally decreased with depth and distance from shore, albeit with contrasting patterns in each submarine canyon (Fig. 6). Noticeably, while terrigenous OC deposited in marine systems can be comprised of biogenic OC (e.g., plants, leaves, soil) and petrogenic OC (e.g., bedrock weathering) (Galy et al., 2008; Kao et al., 2014; Kim et al., 2022), the  $^{14}\text{C}$  fraction modern mixing model as exemplified by Galy et al. (2008) (Fig. S7) indicates that OC in this system mostly appears to consist of biogenic OC, with negligible contribution of petrogenic OC. This is probably due to the limited presence of petrogenic OC from the lithology surrounding the hills of Palermo despite the high erodibility of soils in this area (Fantappiè et al., 2015), which have been shown to be decisive factors in the weathering of petrogenic OC (Evans et al., 2025). Moreover, the radiocarbon age

of OC in surface sediments from the Gulf of Palermo, ranging between 1900 and 2600 yr BP (Fig. S2b), is similar to those of surficial sediments from other continental margins that are not influenced by petrogenic input (Paradis et al., 2023, 2024). To identify the different origins of terrigenous OC (i.e., soil-derived or plant-derived), we assessed spatial variations of soil-derived GDGT proxies and plant-derived high molecular weight fatty acids (HMW FA).

The BIT index, the ratio of brGDGTs and isoGDGTs, is often employed as a proxy of soil-derived terrigenous contribution, where a high BIT index ( $> 0.6$ ) is indicative of high input of soil-derived OM (Hopmans et al., 2004; Weijers et al., 2014). However, the BIT index was low throughout the study area, ranging only from 0.025–0.050, contrasting sharply with values of 0.6–0.8 in sites offshore river mouths on other continental margins (Kim et al., 2006; Yedema et al., 2023), indicating limited input of soil-derived terrigenous OC. In addition, brGDGTs from the Gulf of Palermo had very distinct composition than those of global soils and peats (Dearing Crampton-Flood et al., 2020) (Fig. S8), indicating that brGDGTs in surficial sediment from the Gulf of Palermo may not necessarily reflect terrigenous soil contributions. Hence, analyses of other soil-derived biomarkers (Tesi et al., 2008; Kim et al., 2022; Paradis et al., 2022) might be more informative to determine the contribution of soil OM in this system.

In the case of plant-derived HMW FA, highest concentrations were observed on the shelf (S-70), as expected, given its proximity to the coast and the Oreto river mouth (Fig. 4c). Similarly high concentrations of HMW FA were also observed in Arenella mid-canyon (AC-500), suggesting that, although this site has lowest terrigenous OC content ( $\sim 0.6\%$ ) in comparison to the other canyon sites (0.6–0.8%), it has the highest plant-derived OC ( $25 \mu\text{g g}^{-1}$  OC) relative to the other canyons ( $18\text{--}21 \mu\text{g g}^{-1}$  OC), with the exception of Oreto canyon mouth (OC-800) (see Sect. 4.3). This points to a distinct source of terrigenous OC deposited in this canyon in comparison to the other canyons in this gulf. This is further supported by the contrasting OM composition in terms of proteins, carbohydrates and lipids, since Arenella Canyon had the highest lipid contents but lowest proteins and carbohydrate contents in comparison to the other canyons (Fig. 3).

#### 4.3 Dispersal of terrigenous organic carbon in the Gulf of Palermo

Despite the general offshore decrease of terrigenous OC across the Gulf of Palermo, each canyon exhibited distinct patterns and specific sources of terrigenous OC, which we attribute to the influence of dispersal mechanisms of terrigenous OC: Arenella Canyon located up-current had lowest terrigenous OC fraction but highest land plant-derived OC contents, Oreto Canyon located in the middle part of the gulf presented a down-canyon increase of both terrigenous OC fraction and plant-derived OC, whereas Eleuterio Canyon lo-

cated farther down-current and closest to the coast and rivers had highest terrigenous OC fraction but lowest plant-derived OC.

To better understand the dispersal of terrigenous OC in the Gulf of Palermo, we examine the  $\delta^{13}\text{C}$  compositions of individual fatty acids (Fig. 5). Although always more  $^{13}\text{C}$ -depleted than the corresponding bulk  $\delta^{13}\text{C}$  signatures,  $\delta^{13}\text{C}$  values are usually higher in the low carbon number fatty acids since these generally represent marine OM, whereas terrigenous fatty acids with higher carbon number tend to have lower  $\delta^{13}\text{C}$  values, echoing terrigenous  $\delta^{13}\text{C}$  signatures (e.g., Tao et al., 2016). However, this is not the case across the Gulf of Palermo. As expected, we observe a general decrease in  $\delta^{13}\text{C}$  values with increasing carbon number between  $\text{C}_{16}$  and  $\text{C}_{20}$  (LMW FA representative of marine OM). However, this trend is reversed in the  $\text{C}_{24}$  to  $\text{C}_{28}$  fatty acids (HMW FA of terrigenous origin) (Fig. 5). In fact, we observe two distinct trends in the  $\delta^{13}\text{C}$  signatures of HMW FA: sediment cores collected on the shelf and in Eleuterio Canyon exhibit a modest 0.9‰ increase of  $\delta^{13}\text{C}$  values with increasing fatty acid carbon number ( $\text{C}_{24}$  to  $\text{C}_{28}$ ), whereas the sediment cores collected in Oreto and Arenella canyons presented a larger 3.4‰ increase. This difference in the  $\delta^{13}\text{C}$  signatures of HMW FA implies distinct sources of terrigenous OM in surficial sediment across the Gulf of Palermo.

The variation of weighted-average  $\delta^{13}\text{C}$  values of HMW FAs is consistent with the eastward direction of the regional current, with higher values observed in Arenella Canyon ( $-26.3 \pm 0.3\text{‰}$ ), slightly lower  $\delta^{13}\text{C}$  values of HMW FA reaching Oreto Canyon ( $-27.4 \pm 0.2\text{‰}$ ), and lowest  $\delta^{13}\text{C}$  values of HMW FA deposited in Eleuterio Canyon ( $-29.2 \pm 0.5\text{‰}$ ), similar to the signature on the shelf ( $-29.2 \pm 0.2\text{‰}$ ) (Fig. 4d). This pattern suggests that terrigenous OC delivered by both Oreto and Eleuterio rivers are transported eastwards until reaching Cape Zafferano, where this promontory then redirects currents towards the head of Eleuterio Canyon located approximately 2 km offshore, thereby transferring larger amounts of terrigenous OC from these rivers into this canyon (Fig. 8). This agrees with the higher natural (i.e., unaffected by bottom trawling)  $^{210}\text{Pb}$ -derived sedimentation rate observed in EC-200 (Paradis et al., 2021). In contrast, terrigenous OC reaching Arenella Canyon would originate from a different source farther up-current from the Gulf of Palermo (e.g., distal rivers such as those that discharge into the adjacent Gulf of Castellammare, aeolian input, or coastal erosion). Finally, the slightly lower weighted-average  $\delta^{13}\text{C}$  signature of HMW FAs in Oreto Canyon in comparison to Arenella Canyon (Fig. 4d) suggests that the terrigenous OC that reaches this canyon is a mixture of the allochthonous terrigenous OC that reaches Arenella Canyon and those delivered by the Oreto River. Using the weighted-average  $\delta^{13}\text{C}$  signature of HMW FAs from the shelf and Arenella Canyon as possible end-members of local riverine and distal terrigenous OC source, respectively, only 30%–40% of the terrigenous OC delivered by the Oreto

River would be deposited in the Oreto Canyon, whereas the majority would originate from another up-current source that this canyon intercepts (Fig. 8). However, additional sampling should be conducted to further refine the endmembers used in this study area (Table 1) and provide more definite understanding of the dispersal of terrigenous and marine OC in the Gulf of Palermo, such as sampling the different rivers and collecting suspended particles to determine marine OC signatures.

A similar pattern was observed in the submarine canyons of New Zealand, where  $\delta^{13}\text{C}$  analysis of fatty acids revealed that terrigenous OC deposited in submarine canyons did not originate from the closest river, but rather from more distal rivers which were transported by longshore drift and intercepted by the canyon (Gibbs et al., 2020). This highlights the importance of coastal sedimentary dynamics in distributing terrigenous OC into submarine canyons. In addition, the spatial variation in  $\text{CPI}_{(\text{C}_{24}-\text{C}_{32})}$  values of HMW FA across canyons (Fig. S3f), a metric of the degree of degradation of plant-derived OC, points to more degraded HMW FAs deposited in Arenella Canyon, slightly less degraded HMW FAs deposited in Oreto Canyon, and least degraded HMW FAs deposited in Eleuterio Canyon, consistent with the transit of terrigenous OC through the system (Fig. 8). It is important to note that these  $\text{CPI}_{(\text{C}_{24}-\text{C}_{32})}$  values (1.8–2.4) are lower than those observed in other continental margins with significant riverine input as well as high HMW FA contents in surficial sediments, such as East China Sea ( $400\text{--}900\ \mu\text{g g}^{-1}$  OC,  $\text{CPI}_{(\text{C}_{24}-\text{C}_{32})}$  3.4–4.7; Tao et al., 2016), the Laptev Sea ( $300\text{--}7150\ \mu\text{g g}^{-1}$  OC,  $\text{CPI}_{(\text{C}_{24}-\text{C}_{32})}$  3.7–5.9; Bröder et al., 2016), and the Helgoland Mud Area in the North Sea ( $170\text{--}1150\ \mu\text{g g}^{-1}$  OC,  $\text{CPI}_{(\text{C}_{24}-\text{C}_{32})}$  4–5.5; Wei et al., 2025), indicating that the limited plant-derived OM deposited in the Gulf of Palermo is already considerably degraded, which could be a characteristic of continental margins affected by ephemeral, torrential rivers.

The dispersal of terrigenous OM is not only affected by the regional currents, but also by trawling-derived sediment resuspension, both of which displace large amounts of sediment from the shelf and slope into these submarine canyons (Paradis et al., 2021; Arjona-Camas et al., 2024). This transfer of sediment into submarine canyons has not only increased sedimentation rates within all three canyons since the industrialization of the bottom trawling fishing fleet in the 1980s (Paradis et al., 2021), but it has contributed to the dilution of heavy metals accumulating in the canyons (Palanques et al., 2022). Hence, this anthropogenically-induced sediment transport could also be affecting the dispersal of terrigenous and marine OC in the Gulf of Palermo submarine canyons, delivering more resuspended OC into the canyons (Fig. 8). In addition, the higher sedimentation rates in submarine canyons associated to sediment resuspension by bottom trawling activities on the flanks could be increasing the preservation potential of OC within submarine canyons, and further studies should address this.

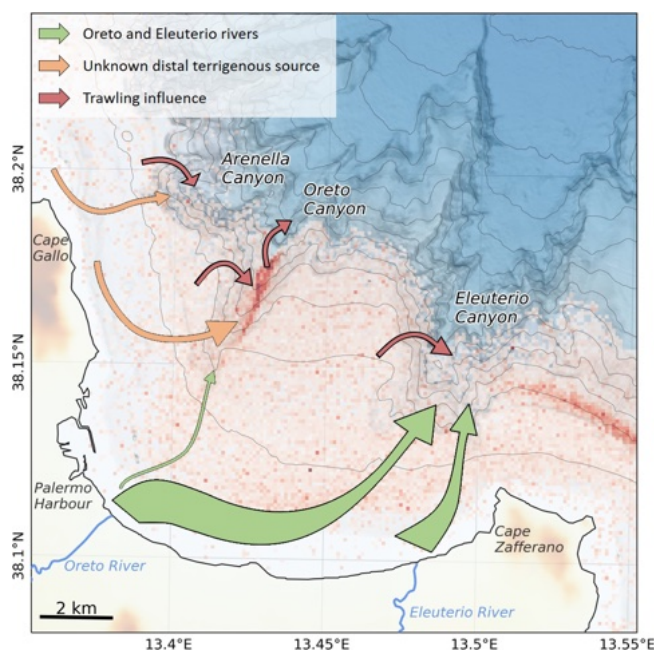


**Figure 8.** Schematic diagram of the dispersal pathways of terrigenous OM across the shelf of the Gulf of Palermo and its submarine canyons. The colour of the arrows indicates distinct terrigenous OM sources or dispersal mechanism whereas the size represents the magnitude of the terrigenous OM transported.

Bottom trawling activities could also be affecting OC content and composition. This would be the case in the Oreto Canyon, where bottom trawlers continuously fish along the canyon axis and highest fishing effort of the region have been recorded in this canyon (Fig. 8). Here, the repetitive resuspension and down-canyon transport of sediment and OC could explain the down-canyon increase of terrigenous OC and plant-derived (HMW FA) OC along this canyon (Figs. 4c, 6). Furthermore, the continuous sediment resuspension and erosion at this site (OC-500) due to repetitive bottom trawling promotes a reduction of OC contents in surficial sediment (Tiano et al., 2024), either associated to erosion or degradation of OC. Given the high sedimentation rates in this site (Paradis et al., 2021), it is unlikely that the reduction of OC associated to bottom trawling in this site is due to erosion, but it may rather be dominated by enhanced degradation of OC, potentially due to sediment mixing (e.g., Middelburg, 2018) and oxygenation (e.g., increasing oxygen exposure time of OC (Hartnett et al., 1998), depleting the most reactive OM components such as phytopigments from the seafloor (Fig. 3d). This process shifts the OC source toward less marine and more terrigenous OC, which tend to be less reactive, as seen by the low protein turnover rate in this site (Figs. 3d, S2c). This process leads to older (i.e., more  $^{14}\text{C}$ -depleted) and less reactive OC on surface sediments, which could impair ecosystem functioning (Danovaro et al., 2008) in this area, ultimately affecting benthic community

composition and abundance (Pusceddu et al., 2014; Good et al., 2022).

## 5 Conclusions

The contribution of terrigenous and marine OC in the Gulf of Palermo continental shelf and submarine canyon system was determined using multiple proxies and mixing models. Highest marine OC contents were found in Arenella Canyon, and shown to be primarily of phytoplankton origin, while in the Oreto canyon head, marine OC consisting of a combination of phytoplankton and microbial inputs. The terrigenous OC contents decreased offshore, being highest on the continental shelf and lowest in the submarine canyons. However, terrigenous OC accumulation rates were highest in all the studied submarine canyons, highlighting their role in funnelling and sequestering terrigenous OC. The BIT ratio based on GDGT distributions indicate that soil OC inputs are low. In contrast, using compound-specific  $\delta^{13}\text{C}$  plant-derived FAs, we were able to identify two predominant sources of terrigenous OC across the Gulf of Palermo: terrigenous OC exported from the Oreto and Eleuterio rivers that discharge into the Gulf of Palermo, and terrigenous OC supply from a distal source, likely via along margin advective transport. The distribution of these two terrigenous sources was linked to the dispersal pathway of terrigenous OC, which was governed by the main regional currents: Arenella Canyon located farther up-current received terrigenous OC from a distal source, Oreto Canyon received a combination of distal and local riverine terrigenous OC, while Eleuterio Canyon, located farther down-current at the edge of the gulf, likely received local terrigenous OC exclusively from Oreto and Eleuterio rivers. Finally, anthropogenic sediment disturbance caused by bottom trawling also plays a role in the distribution of terrigenous OC, promoting the down-canyon transport of terrigenous OC. The repeated trawling-induced sediment resuspension and erosion reduces the availability of fresh organic matter, leading to aged OC and potentially affecting ecosystem functioning. Our findings emphasize the need to consider hydrodynamic and sedimentary transport processes to understand the dispersal of terrigenous OC across continental margins. We also highlight that non-river connected canyons can serve as important sites in the sequestration of terrigenous OC. This is especially significant given that the majority of submarine canyons nowadays are not connected to a river, yet they could still be important in sequestering terrigenous OM transported by along-margin currents and transferring it towards deeper environments.

*Data availability.* All the data used to produce this study are available in Paradis (2025).

*Supplement.* The supplement related to this article is available online at <https://doi.org/10.5194/bg-22-5921-2025-supplement>.

*Author contributions.* SP, AnP, PP, CLI, and TE designed the scientific study. SP and CLI retrieved the samples. NH analyzed the isotopic composition of the samples. SP analyzed mineral surface area. SP and DM analyzed proteins, carbohydrates, lipids, and phytopigments. SP and HG analyzed fatty acids and glycerol dialkyl glycerol tetraethers. JL performed the compound-specific isotopic analysis of fatty acids. HG, JL, LB contributed to the data processing of all biomarkers. All authors contributed to the data interpretation and SP wrote the manuscript with the contribution of all co-authors.

*Competing interests.* The contact author has declared that none of the authors has any competing interests.

*Disclaimer.* Publisher's note: Copernicus Publications remains neutral with regard to jurisdictional claims made in the text, published maps, institutional affiliations, or any other geographical representation in this paper. While Copernicus Publications makes every effort to include appropriate place names, the final responsibility lies with the authors. Also, please note that this paper has not received English language copy-editing. Views expressed in the text are those of the authors and do not necessarily reflect the views of the publisher.

*Acknowledgements.* The samples were obtained within the Exploring SiciLian CANYoN Dynamics (ISLAND) research cruise supported by the European Commission, Seventh Framework Programme (EUROFLEETS2; 312762). We would like to thank R. Wijker and T. M. Blattmann from ETH Zurich for their assistance with the compound-specific carbon isotopic analyses and the correct functioning of analytical laboratory equipment, respectively. Albert Palanques, Pere Puig and Claudio Lo Iacono belong to CRG on Littoral and Oceanic Processes, Grant 2021 SGR 433 provided by the Generalitat de Catalunya. This work is contributing to the ICM "Center of Excellence" Severo Ochoa grant (CEX2024-001494-S) funded by AEI 10.13039/501100011033.

*Financial support.* This research has been supported by the Seventh Framework Programme, FP7 Capacities (grant no. EUROFLEETS2; 312762), the Agencia Estatal de Investigación (grant no. ABIDES; CTM2015-65142-R), the ETH Zürich Foundation (grant no. FACTS; SEED-25 21-2), and the Schweizerischer Nationalfonds zur Förderung der Wissenschaftlichen Forschung (grant nos. CAPS-LOCK3; SNF200020\_184865/1, CAPS-LOCK+, SNF200020\_215163, and PZ00P2\_223468).

*Review statement.* This paper was edited by Jack Middelburg and reviewed by four anonymous referees.

## References

- Abril-Pla, O., Andreani, V., Carroll, C., Dong, L., Fomesbeck, C. J., Kochurov, M., Kumar, R., Lao, J., Luhmann, C. C., Martin, O. A., Osthege, M., Vieira, R., Wiecki, T., and Zinkov, R.: PyMC: a modern, and comprehensive probabilistic programming framework in Python, *PeerJ Comput. Sci.*, 9, e1516, <https://doi.org/10.7717/peerj-cs.1516>, 2023.
- Alt-Epping, U., Mil-Homens, M., Hebbeln, D., Abrantes, F., and Schneider, R. R.: Provenance of organic matter and nutrient conditions on a river- and upwelling influenced shelf: A case study from the Portuguese Margin, *Mar. Geol.*, 243, 169–179, <https://doi.org/10.1016/j.margeo.2007.04.016>, 2007.
- Amundson, R., Austin, A. T., Schuur, E. A. G., Yoo, K., Matzek, V., Kendall, C., Uebersax, A., Brenner, D., and Baisden, W. T.: Global patterns of the isotopic composition of soil and plant nitrogen, *Global Biogeochem. Cycles*, 17, <https://doi.org/10.1029/2002GB001903>, 2003.
- Andersson, A.: A systematic examination of a random sampling strategy for source apportionment calculations, *Sci. Total Environ.*, 412/413, 232–238, <https://doi.org/10.1016/j.scitotenv.2011.10.031>, 2011.
- Arjona-Camas, M., Lo Iacono, C., Puig, P., Russo, T., and Palanques, A.: Trawling-Induced Sedimentary Dynamics in Submarine Canyons of the Gulf of Palermo (SW Mediterranean Sea), *J. Mar. Sci. Eng.*, 12, 1050, <https://doi.org/10.3390/jmse12071050>, 2024.
- Ausín, B., Bossert, G., Krake, N., Paradis, S., Haghypour, N., Durrieu de Madron, X., Alonso, B., and Eglinton, T.: Sources and fate of sedimentary organic matter in the Western Mediterranean Sea, *Global Biogeochem. Cy.*, <https://doi.org/10.1029/2023GB007695>, 2023.
- Baker, M. L., Hage, S., Talling, P. J., Acikalin, S., Hilton, R. G., Haghypour, N., Ruffell, S. C., Pope, E. L., Jacinto, R. S., Clare, M. A., and Sahin, S.: Globally significant mass of terrestrial organic carbon efficiently transported by canyon-flushing turbidity currents, *Geology*, 52, 631–636, <https://doi.org/10.1130/G51976.1>, 2024.
- Bao, R., McIntyre, C., Zhao, M., Zhu, C., Kao, S.-J., and Eglinton, T. I.: Widespread dispersal and aging of organic carbon in shallow marginal seas, *Geology*, 44, 791–794, <https://doi.org/10.1130/G37948.1>, 2016.
- Bao, R., van der Voort, T. S., Zhao, M., Guo, X., Montluçon, D. B., McIntyre, C., and Eglinton, T. I.: Influence of Hydrodynamic Processes on the Fate of Sedimentary Organic Matter on Continental Margins, *Global Biogeochem. Cy.*, 32, 1420–1432, <https://doi.org/10.1029/2018GB005921>, 2018.
- Bao, R., Blattmann, T. M., McIntyre, C., Zhao, M., and Eglinton, T. I.: Relationships between grain size and organic carbon  $^{14}\text{C}$  heterogeneity in continental margin sediments, *Earth Planet. Sc. Lett.*, 505, 76–85, <https://doi.org/10.1016/j.epsl.2018.10.013>, 2019.
- Baudin, F., Rabouille, C., and Dennielou, B.: Routing of terrestrial organic matter from the Congo River to the ultimate sink in the abyss: a mass balance approach (André Dumont medallist lecture 2017), *Geol. Belgica*, 23, <https://doi.org/10.20341/gb.2020.004>, 2020.
- Bender, M. M.: Variations in the  $^{13}\text{C}/^{12}\text{C}$  ratios of plants in relation to the pathway of photosynthetic carbon dioxide fixation, *Phytochemistry*, 10, 1239–1244, [https://doi.org/10.1016/S0031-9422\(00\)84324-1](https://doi.org/10.1016/S0031-9422(00)84324-1), 1971.
- Billi, P. and Fazzini, M.: Global change and river flow in Italy, *Glob. Planet. Change*, 155, 234–246, <https://doi.org/10.1016/j.gloplacha.2017.07.008>, 2017.
- Blair, N. E. and Aller, R. C.: The Fate of Terrestrial Organic Carbon in the Marine Environment, *Ann. Rev. Mar. Sci.*, 4, 401–423, <https://doi.org/10.1146/annurev-marine-120709-142717>, 2012.
- Bligh, E. G. and Dyer, W. J.: A rapid method of total lipid extraction and purification, *Can. J. Biochem. Physiol.*, 37, 911–917, <https://doi.org/10.1139/o59-099>, 1959.
- Bray, E. and Evans, E. : Distribution of n-paraffins as a clue to recognition of source beds, *Geochim. Cosmochim. Ac.*, 22, 2–15, [https://doi.org/10.1016/0016-7037\(61\)90069-2](https://doi.org/10.1016/0016-7037(61)90069-2), 1961.
- Briggs, R. A., Ruttnerberg, K. C., Glazer, B. T., and Ricardo, A. E.: Constraining Sources of Organic Matter to Tropical Coastal Sediments: Consideration of Nontraditional End-members, *Aquat. Geochem.*, 19, 543–563, <https://doi.org/10.1007/s10498-013-9219-2>, 2013.
- Bröder, L., Tesi, T., Salvadó, J. A., Semiletov, I. P., Dudarev, O. V., and Gustafsson, Ö.: Fate of terrigenous organic matter across the Laptev Sea from the mouth of the Lena River to the deep sea of the Arctic interior, *Biogeosciences*, 13, 5003–5019, <https://doi.org/10.5194/bg-13-5003-2016>, 2016.
- Bröder, L., Tesi, T., Andersson, A., Semiletov, I., and Gustafsson, Ö.: Bounding cross-shelf transport time and degradation in Siberian-Arctic land-ocean carbon transfer, *Nat. Commun.*, 9, 806, <https://doi.org/10.1038/s41467-018-03192-1>, 2018.
- Brunauer, S., Emmett, P. H., and Teller, E.: Adsorption of Gases in Multimolecular Layers, *J. Am. Chem. Soc.*, 60, 309–319, <https://doi.org/10.1021/ja01269a023>, 1938.
- Burdige, D. J.: Burial of terrestrial organic matter in marine sediments: A re-assessment, *Global Biogeochem. Cy.*, 19, GB4011, <https://doi.org/10.1029/2004GB002368>, 2005.
- Buscail, R., Ambatsian, P., Monaco, A., and Bernat, M.: 210Pb, manganese and carbon: Indicators of focusing processes on the northwestern Mediterranean continental margin, *Mar. Geol.*, 137, 271–286, [https://doi.org/10.1016/S0025-3227\(96\)00055-2](https://doi.org/10.1016/S0025-3227(96)00055-2), 1997.
- Campanyà-Llovet, N., Snelgrove, P. V. R., and De Leo, F. C.: Food quantity and quality in Barkley Canyon (NE Pacific) and its influence on macrofaunal community structure, *Prog. Oceanogr.*, 169, 106–119, <https://doi.org/10.1016/j.pocean.2018.04.003>, 2018.
- Danovaro, R.: Methods for the Study of Deep-Sea Sediments, Their Functioning and Biodiversity, 1st Editio., edited by: Danovaro, R., CRC Press, Boca Raton, 458 pp., <https://doi.org/10.1201/9781439811382>, 2009.
- Danovaro, R., Gambi, C., Dell'Anno, A., Corinaldesi, C., Fraschetti, S., Vanreusel, A., Vincx, M., and Gooday, A. J.: Exponential Decline of Deep-Sea Ecosystem Functioning Linked to Benthic Biodiversity Loss, *Curr. Biol.*, 18, 1–8, <https://doi.org/10.1016/j.cub.2007.11.056>, 2008.
- Dearing Crampton-Flood, E., Tierney, J. E., Peterse, F., Kirkels, F. M. S. A., and Sinninghe Damsté, J. S.: BayMBT: A Bayesian calibration model for branched glycerol dialkyl glycerol tetraethers in soils and peats, *Geochim. Cosmochim. Ac.*, 268, 142–159, <https://doi.org/10.1016/j.gca.2019.09.043>, 2020.

- Deegan, L. and Garritt, R.: Evidence for spatial variability in estuarine food webs, *Mar. Ecol. Prog. Ser.*, 147, 31–47, <https://doi.org/10.3354/meps147031>, 1997.
- De Leo, F. C., Smith, C. R., Rowden, A. A., Bowden, D. A., and Clark, M. R.: Submarine canyons: hotspots of benthic biomass and productivity in the deep sea, *Proc. R. Soc. B Biol. Sci.*, 277, 2783–2792, <https://doi.org/10.1098/rspb.2010.0462>, 2010.
- Dell’Anno, A., Pusceddu, A., Corinaldesi, C., Canals, M., Heussner, S., Thomsen, L., and Danovaro, R.: Trophic state of benthic deep-sea ecosystems from two different continental margins off Iberia, *Biogeosciences*, 10, 2945–2957, <https://doi.org/10.5194/bg-10-2945-2013>, 2013.
- Di Leonardo, R., Vizzini, S., Bellanca, A., and Mazzola, A.: Sedimentary record of anthropogenic contaminants (trace metals and PAHs) and organic matter in a Mediterranean coastal area (Gulf of Palermo, Italy), *J. Mar. Syst.*, 78, 136–145, <https://doi.org/10.1016/j.jmarsys.2009.04.004>, 2009.
- Di Leonardo, R., Bellanca, A., Capotondi, L., Cundy, A., and Neri, R.: Possible impacts of Hg and PAH contamination on benthic foraminiferal assemblages: An example from the Sicilian coast, central Mediterranean, *Sci. Total Environ.*, 388, 168–183, <https://doi.org/10.1016/j.scitotenv.2007.08.009>, 2007.
- Di Leonardo, R., Cundy, A. B., Bellanca, A., Mazzola, A., and Vizzini, S.: Biogeochemical evaluation of historical sediment contamination in the Gulf of Palermo (NW Sicily): Analysis of pseudo-trace elements and stable isotope signals, *J. Mar. Syst.*, 94, 185–196, <https://doi.org/10.1016/j.jmarsys.2011.11.022>, 2012.
- Domina, G., Barone, G., and Gianguzzi, L.: The flora of the Natura 2000 site “ITA020006 – Capo Gallo” (NW Sicily, Italy) and the effects of fire to its composition, *Plant Biosyst. - An Int. J. Deal. with all Asp. Plant Biol.*, 1–17, <https://doi.org/10.1080/11263504.2025.2479492>, 2025.
- Eglinton, G. and Hamilton, R. J.: Leaf Epicuticular Waxes, *Science*, 156, 1322–1335, <https://doi.org/10.1126/science.156.3780.1322>, 1967.
- Evans, D. L., Doetterl, S., Gallarotti, N., Georgiadis, E., Nabhan, S., Wartenweiler, S. H., Rhyner, T. M. Y., Mittelbach, B. V. A., Eglinton, T. I., Hemingway, J. D., and Blattmann, T. M.: The Known Unknowns of Petrogenic Organic Carbon in Soils, *AGU Adv.*, 6, <https://doi.org/10.1029/2024AV001625>, 2025.
- Fabiano, M. and Danovaro, R.: Enzymatic activity, bacterial distribution, and organic matter composition in sediments of the Ross Sea (Antarctica), *Appl. Environ. Microbiol.*, 64, 3838–3845, 1998.
- Fabiano, M., Danovaro, R., and Frascchetti, S.: A three-year time series of elemental and biochemical composition of organic matter in subtidal sandy sediments of the Ligurian Sea (northwestern Mediterranean), *Cont. Shelf Res.*, 15, 1453–1469, [https://doi.org/10.1016/0278-4343\(94\)00088-5](https://doi.org/10.1016/0278-4343(94)00088-5), 1995.
- Fantappiè, M., Priori, S., and Costantini, E. A. C.: Soil erosion risk, Sicilian Region (1:250,000 scale), *J. Maps*, 11, 323–341, <https://doi.org/10.1080/17445647.2014.956349>, 2015.
- Farquhar, G. D., Ehleringer, J. R., and Hubick, K. T.: Carbon Isotope Discrimination and Photosynthesis, *Annu. Rev. Plant Physiol. Plant Mol. Biol.*, 40, 503–537, <https://doi.org/10.1146/annurev.pp.40.060189.002443>, 1989.
- Fernandez-Arcaya, U., Ramirez-Llodra, E., Aguzzi, J., Allcock, A. L., Davies, J. S., Dissanayake, A., Harris, P., Howell, K., Huvenne, V. A. I., Macmillan-Lawler, M., Martín, J., Menot, L., Nizinski, M., Puig, P., Rowden, A. A., Sanchez, F., and Van den Beld, I. M. J.: Ecological Role of Submarine Canyons and Need for Canyon Conservation: A Review, *Front. Mar. Sci.*, 4, 5, <https://doi.org/10.3389/fmars.2017.00005>, 2017.
- Galy, V., Beyssac, O., France-Lanord, C., and Eglinton, T.: Recycling of Graphite During Himalayan Erosion: A Geological Stabilization of Carbon in the Crust, *Science*, 322, 943–945, <https://doi.org/10.1126/science.1161408>, 2008.
- Gambi, C., Pusceddu, A., Benedetti-Cecchi, L., and Danovaro, R.: Species richness, species turnover and functional diversity in nematodes of the deep Mediterranean Sea: searching for drivers at different spatial scales, *Glob. Ecol. Biogeogr.*, 23, 24–39, <https://doi.org/10.1111/geb.12094>, 2014.
- Gambi, C., Corinaldesi, C., Dell’Anno, A., Pusceddu, A., D’Onghia, G., Covazzi-Harriague, A., and Danovaro, R.: Functional response to food limitation can reduce the impact of global change in the deep-sea benthos, *Glob. Ecol. Biogeogr.*, 26, 1008–1021, <https://doi.org/10.1111/geb.12608>, 2017.
- Gerchakov, S. M. and Hatcher, P. G.: Improved technique for analysis of carbohydrates in sediments, *Limnol. Oceanogr.*, 17, 938–943, <https://doi.org/10.4319/lo.1972.17.6.0938>, 1972.
- Gibbs, M., Leduc, D., Nodder, S. D., Kingston, A., Swales, A., Rowden, A. A., Mountjoy, J., Olsen, G., Oviden, R., Brown, J., Bury, S., and Graham, B.: Novel Application of a Compound-Specific Stable Isotope (CSSI) Tracking Technique Demonstrates Connectivity Between Terrestrial and Deep-Sea Ecosystems via Submarine Canyons, *Front. Mar. Sci.*, 7, <https://doi.org/10.3389/fmars.2020.00608>, 2020.
- Goñi, M. A., Ruttenger, K. C., and Eglinton, T. I.: A reassessment of the sources and importance of land-derived organic matter in surface sediments from the Gulf of Mexico, *Geochim. Cosmochim. Ac.*, 62, 3055–3075, [https://doi.org/10.1016/S0016-7037\(98\)00217-8](https://doi.org/10.1016/S0016-7037(98)00217-8), 1998.
- Goñi, M. A., O’Connor, A. E., Kuzyk, Z. Z., Yunker, M. B., Gobiel, C., and Macdonald, R. W.: Distribution and sources of organic matter in surface marine sediments across the North American Arctic margin, *J. Geophys. Res.-Ocean.*, 118, 4017–4035, <https://doi.org/10.1002/jgrc.20286>, 2013.
- Goñi, M. A., Moore, E., Kurtz, A., Portier, E., Alleau, Y., and Merrell, D.: Organic matter compositions and loadings in soils and sediments along the Fly River, Papua New Guinea, *Geochim. Cosmochim. Ac.*, 140, 275–296, <https://doi.org/10.1016/J.GCA.2014.05.034>, 2014.
- Good, E., Holman, L. E., Pusceddu, A., Russo, T., Rius, M., and Lo Iacono, C.: Detection of community-wide impacts of bottom trawl fishing on deep-sea assemblages using environmental DNA metabarcoding, *Mar. Pollut. Bull.*, 183, 114062, <https://doi.org/10.1016/j.marpolbul.2022.114062>, 2022.
- Gordon, E. S. and Goñi, M. A.: Sources and distribution of terrigenous organic matter delivered by the Atchafalaya River to sediments in the northern Gulf of Mexico, *Geochim. Cosmochim. Ac.*, 67, 2359–2375, [https://doi.org/10.1016/S0016-7037\(02\)01412-6](https://doi.org/10.1016/S0016-7037(02)01412-6), 2003.
- Harmelin-Vivien, M., Loizeau, V., Mellon, C., Beker, B., Arlhac, D., Bodiguel, X., Ferraton, F., Hermand, R., Philippon, X., and Salen-Picard, C.: Comparison of C and N stable isotope ratios between surface particulate organic matter and microphytoplankton

- in the Gulf of Lions (NW Mediterranean), *Cont. Shelf Res.*, 28, 1911–1919, <https://doi.org/10.1016/j.csr.2008.03.002>, 2008.
- Hartnett, H. E., Keil, R. G., Hedges, J. I., and Devol, A. H.: Influence of oxygen exposure time on organic carbon preservation in continental margin sediments, *Nature*, 391, 572–575, <https://doi.org/10.1038/35351>, 1998.
- Hartree, E. F.: Determination of protein: A modification of the lowry method that gives a linear photometric response, *Anal. Biochem.*, 48, 422–427, [https://doi.org/10.1016/0003-2697\(72\)90094-2](https://doi.org/10.1016/0003-2697(72)90094-2), 1972.
- Hedges, J. I. and Keil, R. G.: Sedimentary organic matter preservation: an assessment and speculative synthesis, *Mar. Chem.*, 49, 81–115, [https://doi.org/10.1016/0304-4203\(95\)00008-F](https://doi.org/10.1016/0304-4203(95)00008-F), 1995.
- Hopmans, E. C., Weijers, J. W., Schefuß, E., Herfort, L., Sinninghe Damsté, J. S., and Schouten, S.: A novel proxy for terrestrial organic matter in sediments based on branched and isoprenoid tetraether lipids, *Earth Planet. Sci. Lett.*, 224, 107–116, <https://doi.org/10.1016/j.epsl.2004.05.012>, 2004.
- Hopmans, E. C., Schouten, S., and Sinninghe Damsté, J. S.: The effect of improved chromatography on GDGT-based palaeoproxies, *Org. Geochem.*, 93, 1–6, <https://doi.org/10.1016/j.orggeochem.2015.12.006>, 2016.
- Hsu, F.-H., Su, C.-C., Wang, C.-H., Lin, S., Liu, J., and Huh, C.-A.: Accumulation of terrestrial organic carbon on an active continental margin offshore southwestern Taiwan: Source-to-sink pathways of river-borne organic particles, *J. Asian Earth Sci.*, 91, 163–173, <https://doi.org/10.1016/j.jseas.2014.05.006>, 2014.
- Huguet, C., Hopmans, E. C., Febo-Ayala, W., Thompson, D. H., Sinninghe Damsté, J. S., and Schouten, S.: An improved method to determine the absolute abundance of glycerol dibiphytanyl glycerol tetraether lipids, *Org. Geochem.*, 37, 1036–1041, <https://doi.org/10.1016/j.orggeochem.2006.05.008>, 2006.
- Huh, C. A., Lin, H. L., Lin, S., and Huang, Y. W.: Modern accumulation rates and a budget of sediment off the Gaoping (Kaoping) River, SW Taiwan: A tidal and flood dominated depositional environment around a submarine canyon, *J. Mar. Syst.*, 76, 405–416, <https://doi.org/10.1016/j.jmarsys.2007.07.009>, 2009.
- Istituto Idrografico della Marina: Atlante delle correnti superficiali dei mari italiani, Genova, 45 pp., ISBN 97888113068, 1982.
- Kao, S.-J., Hilton, R. G., Selvaraj, K., Dai, M., Zehetner, F., Huang, J.-C., Hsu, S.-C., Sparkes, R., Liu, J. T., Lee, T.-Y., Yang, J.-Y. T., Galy, A., Xu, X., and Hovius, N.: Preservation of terrestrial organic carbon in marine sediments offshore Taiwan: mountain building and atmospheric carbon dioxide sequestration, *Earth Surf. Dynam.*, 2, 127–139, <https://doi.org/10.5194/esurf-2-127-2014>, 2014.
- Killops, S. and Killops, V.: *Introduction to Organic Geochemistry*, Wiley, <https://doi.org/10.1002/9781118697214>, 2004.
- Kim, D., Kim, J.-H., Tesi, T., Kang, S., Nogarotto, A., Park, K., Lee, D.-H., Jin, Y. K., Shin, K.-H., and Nam, S.-I.: Changes in the burial efficiency and composition of terrestrial organic carbon along the Mackenzie Trough in the Beaufort Sea, *Estuar. Coast. Shelf Sci.*, 275, 107997, <https://doi.org/10.1016/j.ecss.2022.107997>, 2022.
- Kim, J., Schouten, S., Buscail, R., Ludwig, W., Bonnin, J., Sinninghe Damsté, J. S., and Bourrin, F.: Origin and distribution of terrestrial organic matter in the NW Mediterranean (Gulf of Lions): Exploring the newly developed BIT index, *Geochem. Geophys. Geosy.*, 7, <https://doi.org/10.1029/2006GC001306>, 2006.
- Koga, Y., Nishihara, M., Morii, H., and Akagawa-Matsushita, M.: Ether polar lipids of methanogenic bacteria: structures, comparative aspects, and biosyntheses, *Microbiol. Rev.*, 57, 164–182, <https://doi.org/10.1128/mr.57.1.164-182.1993>, 1993.
- Komada, T., Polly, J. A., and Johnson, L.: Transformations of carbon in anoxic marine sediments: Implications from  $\Delta^{14}\text{C}$  and  $\delta^{13}\text{C}$  signatures, *Limnol. Oceanogr.*, 57, 567–581, <https://doi.org/10.4319/lo.2012.57.2.0567>, 2012.
- Kusch, S., Mollenhauer, G., Willmes, C., Hefter, J., Eglinton, T. I., and Galy, V.: Controls on the age of plant waxes in marine sediments – A global synthesis, *Org. Geochem.*, 157, 104259, <https://doi.org/10.1016/j.orggeochem.2021.104259>, 2021.
- Lalonde, K., Vähätalo, A. V., and Gélinas, Y.: Revisiting the disappearance of terrestrial dissolved organic matter in the ocean: a  $\delta^{13}\text{C}$  study, *Biogeosciences*, 11, 3707–3719, <https://doi.org/10.5194/bg-11-3707-2014>, 2014.
- Lawrence, C. R., Beem-Miller, J., Hoyt, A. M., Monroe, G., Sierra, C. A., Stoner, S., Heckman, K., Blankinship, J. C., Crow, S. E., McNicol, G., Trumbore, S., Levine, P. A., Vinduškova, O., Todd-Brown, K., Rasmussen, C., Hicks Pries, C. E., Schädel, C., McFarlane, K., Doetterl, S., Hatté, C., He, Y., Treat, C., Harden, J. W., Torn, M. S., Estop-Aragonés, C., Asefaw Berhe, A., Keiluweit, M., Della Rosa Kuhnén, Á., Marin-Spiotta, E., Plante, A. F., Thompson, A., Shi, Z., Schimel, J. P., Vaughn, L. J. S., von Fromm, S. F., and Wagai, R.: An open-source database for the synthesis of soil radiocarbon data: International Soil Radiocarbon Database (ISRaD) version 1.0, *Earth Syst. Sci. Data*, 12, 61–76, <https://doi.org/10.5194/essd-12-61-2020>, 2020.
- Leduc, D., Nodder, S. D., Rowden, A. A., Gibbs, M., Berkenbusch, K., Wood, A., De Leo, F., Smith, C., Brown, J., Bury, S. J., and Palletin, A.: Structure of infaunal communities in New Zealand submarine canyons is linked to origins of sediment organic matter, *Limnol. Oceanogr.*, 65, 2303–2327, <https://doi.org/10.1002/lno.11454>, 2020.
- Lehmann, M. F., Bernasconi, S. M., Barbieri, A., and McKenzie, J. A.: Preservation of organic matter and alteration of its carbon and nitrogen isotope composition during simulated and in situ early sedimentary diagenesis, *Geochim. Cosmochim. Acta.*, 66, 3573–3584, [https://doi.org/10.1016/S0016-7037\(02\)00968-7](https://doi.org/10.1016/S0016-7037(02)00968-7), 2002.
- Liu, J. T., Hsu, R. T., Hung, J.-J., Chang, Y.-P., Wang, Y.-H., Rendle-Bühning, R. H., Lee, C.-L., Huh, C.-A., and Yang, R. J.: From the highest to the deepest: The Gaoping River–Gaoping Submarine Canyon dispersal system, *Earth-Sci. Rev.*, 153, 274–300, <https://doi.org/10.1016/j.earscirev.2015.10.012>, 2016.
- Lo Iacono, C., Sulli, A., Agate, M., Lo Presti, V., Pepe, F., and Catalano, R.: Submarine canyon morphologies in the Gulf of Palermo (Southern Tyrrhenian Sea) and possible implications for geo-hazard, *Mar. Geophys. Res.*, 32, 127–138, <https://doi.org/10.1007/s11001-011-9118-0>, 2011.
- Lo Iacono, C., Sulli, A., and Agate, M.: Submarine canyons of north-western Sicily (Southern Tyrrhenian Sea): Variability in morphology, sedimentary processes and evolution on a tectonically active margin, *Deep-Sea Res. Pt. II*, 104, 93–105, <https://doi.org/10.1016/J.DSR2.2013.06.018>, 2014.
- Lorenzen, C. and Jeffrey, J.: Determination of chlorophyll in seawater, *Tech. Pap. Mar. Sci.*, 35, 1–20, 1980.
- Maier, K. L., Rosenberger, K. J., Paull, C. K., Gwiazda, R., Gales, J., Lorenson, T., Barry, J. P., Talling, P. J., McGann, M., Xu, J., Lundsten, E., Anderson, K., Litvin, S. Y., Par-

- sons, D. R., Clare, M. A., Simmons, S. M., Sumner, E. J., and Cartigny, M. J. B.: Sediment and organic carbon transport and deposition driven by internal tides along Monterey Canyon, offshore California, *Deep-Sea Res. Pt. I*, 153, 103108, <https://doi.org/10.1016/j.dsr.2019.103108>, 2019.
- Mannina, G. and Viviani, G.: Water quality modelling for ephemeral rivers: Model development and parameter assessment, *J. Hydrol.*, 393, 186–196, <https://doi.org/10.1016/j.jhydrol.2010.08.015>, 2010.
- Marsh, J. B. and Weinstein, D. B.: Simple charring method for determination of lipids, *J. Lipid Res.*, 7, 574–576, 1966.
- Masson, D. G., Huvenne, V. A. I., de Stigter, H. C., Wolff, G. A., Kiriakoulakis, K., Arzola, R. G., and Blackbird, S.: Efficient burial of carbon in a submarine canyon, *Geology*, 38, 831–834, <https://doi.org/10.1130/G30895.1>, 2010.
- Meyers, P. A.: Preservation of elemental and isotopic source identification of sedimentary organic matter, *Chem. Geol.*, 114, 289–302, [https://doi.org/10.1016/0009-2541\(94\)90059-0](https://doi.org/10.1016/0009-2541(94)90059-0), 1994.
- Middelburg, J. J.: Reviews and syntheses: to the bottom of carbon processing at the seafloor, *Biogeosciences*, 15, 413–427, <https://doi.org/10.5194/bg-15-413-2018>, 2018.
- Palanques, A. and Puig, P.: Particle fluxes induced by benthic storms during the 2012 dense shelf water cascading and open sea convection period in the northwestern Mediterranean basin, *Mar. Geol.*, 406, 119–131, <https://doi.org/10.1016/j.margeo.2018.09.010>, 2018.
- Palanques, A., Paradis, S., Puig, P., Masqué, P., and Lo Iacono, C.: Effects of bottom trawling on trace metal contamination of sediments along the submarine canyons of the Gulf of Palermo (southwestern Mediterranean), *Sci. Total Environ.*, 814, 152658, <https://doi.org/10.1016/j.scitotenv.2021.152658>, 2022.
- Paradis, S.: Geochemical composition of surficial sediments in the Gulf of Palermo, ETH Zurich [data set], <https://doi.org/10.3929/ethz-b-000738723>, 2025.
- Paradis, S., Puig, P., Sanchez-Vidal, A., Masqué, P., Garcia-Orellana, J., Calafat, A., and Canals, M.: Spatial distribution of sedimentation-rate increases in Blanes Canyon caused by technification of bottom trawling fleet, *Prog. Oceanogr.*, 169, 241–252, <https://doi.org/10.1016/j.pocean.2018.07.001>, 2018.
- Paradis, S., Lo Iacono, C., Masqué, P., Puig, P., Palanques, A., and Russo, T.: Evidence of large increases in sedimentation rates due to fish trawling in submarine canyons of the Gulf of Palermo (SW Mediterranean), *Mar. Pollut. Bull.*, 172, 112861, <https://doi.org/10.1016/j.marpolbul.2021.112861>, 2021.
- Paradis, S., Arjona-Camas, M., Goñi, M., Palanques, A., Masqué, P., and Puig, P.: Contrasting particle fluxes and composition in a submarine canyon affected by natural sediment transport events and bottom trawling, *Front. Mar. Sci.*, 9, <https://doi.org/10.3389/fmars.2022.1017052>, 2022.
- Paradis, S., Nakajima, K., Van der Voort, T. S., Gies, H., Wildberger, A., Blattmann, T. M., Bröder, L., and Eglinton, T. I.: The Modern Ocean Sediment Archive and Inventory of Carbon (MOSAIC): version 2.0, *Earth Syst. Sci. Data*, 15, 4105–4125, <https://doi.org/10.5194/essd-15-4105-2023>, 2023.
- Paradis, S., Diesing, M., Gies, H., Haghipour, N., Narman, L., Magill, C., Wagner, T., Galy, V. V., Hou, P., Zhao, M., Kim, J.-H., Shin, K.-H., Lin, B., Liu, Z., Wiesner, M. G., Statterger, K., Chen, J., Zhang, J., and Eglinton, T. I.: Unraveling Environmental Forces Shaping Surface Sediment Geochemical “Isodrapes” in the East Asian Marginal Seas, *Global Biogeochem. Cy.*, 38, <https://doi.org/10.1029/2023GB007839>, 2024.
- Pasqual, C., Lee, C., Goñi, M., Tesi, T., Sanchez-Vidal, A., Calafat, A., Canals, M., and Heussner, S.: Use of organic biomarkers to trace the transport of marine and terrigenous organic matter through the southwestern canyons of the Gulf of Lion, *Mar. Chem.*, 126, 1–12, <https://doi.org/10.1016/j.marchem.2011.03.001>, 2011.
- Pasqual, C., Goñi, M. a, Tesi, T., Sanchez-Vidal, A., Calafat, A., and Canals, M.: Composition and provenance of terrigenous organic matter transported along submarine canyons in the Gulf of Lion (NW Mediterranean Sea), *Prog. Oceanogr.*, 118, 81–94, <https://doi.org/10.1016/j.pocean.2013.07.013>, 2013.
- Pedrosa-Pàmies, R., Sanchez-Vidal, A., Calafat, A., Canals, M., and Durán, R.: Impact of storm-induced remobilization on grain size distribution and organic carbon content in sediments from the Blanes Canyon area, NW Mediterranean Sea, *Prog. Oceanogr.*, 118, 122–136, <https://doi.org/10.1016/j.pocean.2013.07.023>, 2013.
- Peterse, F., Kim, J.-H., Schouten, S., Kristensen, D. K., Koç, N., and Sinninghe Damsté, J. S.: Constraints on the application of the MBT/CBT palaeothermometer at high latitude environments (Svalbard, Norway), *Org. Geochem.*, 40, 692–699, <https://doi.org/10.1016/j.orggeochem.2009.03.004>, 2009.
- Pinardi, N. and Masetti, E.: Variability of the large scale general circulation of the Mediterranean Sea from observations and modelling: a review, *Palaeogeogr. Palaeoclimatol.*, 158, 153–173, [https://doi.org/10.1016/S0031-0182\(00\)00048-1](https://doi.org/10.1016/S0031-0182(00)00048-1), 2000.
- Prouty, N. G., Mienis, F., Campbell-Swarzenski, P., Roark, E. B., Davies, A. J., Robertson, C. M., Duineveld, G., Ross, S. W., Rhode, M., and Demopoulos, A. W. J.: Seasonal variability in the source and composition of particulate matter in the depositional zone of Baltimore Canyon, U.S. Mid-Atlantic Bight, *Deep-Sea Res. Pt. I*, 127, 77–89, <https://doi.org/10.1016/j.dsr.2017.08.004>, 2017.
- Pruski, A. M., Stetten, E., Huguet, A., Vétion, G., Wang, H., Senyariçh, C., and Baudin, F.: Fatty acid biomarkers as indicators of organic matter origin and processes in recent turbidites: The case of the terminal lobe complex of the Congo deep-sea fan, *Org. Geochem.*, 173, 104484, <https://doi.org/10.1016/j.orggeochem.2022.104484>, 2022.
- Puig, P., Palanques, A., and Martín, J.: Contemporary sediment-transport processes in submarine canyons., *Ann. Rev. Mar. Sci.*, 6, 53–77, <https://doi.org/10.1146/annurev-marine-010213-135037>, 2014.
- Pusccheddu, A., Bianchelli, S., Canals, M., Sanchez-Vidal, A., Durrieu De Madron, X., Heussner, S., Lykousis, V., de Stigter, H., Trincardi, F., and Danovaro, R.: Organic matter in sediments of canyons and open slopes of the Portuguese, Catalan, Southern Adriatic and Cretan Sea margins, *Deep-Sea Res. Pt. I*, 57, 441–457, <https://doi.org/10.1016/j.dsr.2009.11.008>, 2010.
- Pusccheddu, A., Mea, M., Canals, M., Heussner, S., Durrieu de Madron, X., Sanchez-Vidal, A., Bianchelli, S., Corinaldesi, C., Dell’Anno, A., Thomsen, L., and Danovaro, R.: Major consequences of an intense dense shelf water cascading event on deep-sea benthic trophic conditions and meiofaunal biodiversity, *Biogeosciences*, 10, 2659–2670, <https://doi.org/10.5194/bg-10-2659-2013>, 2013.

- Pusceddu, A., Bianchelli, S., Martin, J., Puig, P., Palanques, A., Masque, P., and Danovaro, R.: Chronic and intensive bottom trawling impairs deep-sea biodiversity and ecosystem functioning, *P. Natl. Acad. Sci. USA*, 111, 8861–8866, <https://doi.org/10.1073/pnas.1405454111>, 2014.
- Ramaswamy, V., Gaye, B., Shirodkar, P. V., Rao, P. S., Chivas, A. R., Wheeler, D., and Thwin, S.: Distribution and sources of organic carbon, nitrogen and their isotopic signatures in sediments from the Ayeyarwady (Irrawaddy) continental shelf, northern Andaman Sea, *Mar. Chem.*, 111, 137–150, <https://doi.org/10.1016/j.marchem.2008.04.006>, 2008.
- Rice, D. L.: The Detritus Nitrogen Problem: New Observations and Perspectives from Organic Geochemistry, *Mar. Ecol. Prog. Ser.*, 9, 153–162, 1982.
- Rizzo, S., Basile, S., Caruso, A., Cosentino, C., Tranchina, L., and Brai, M.: Dating of a Sediment Core by  $^{210}\text{Pb}_{\text{ex}}$  Method and Pb Pollution Chronology in the Palermo Gulf (Italy), *Water. Air. Soil Pollut.*, 202, 109–120, <https://doi.org/10.1007/s11270-008-9961-z>, 2009.
- Romero-Romero, S., Molina-Ramírez, A., Höfer, J., Duineveld, G., Rumín-Caparrós, A., Sanchez-Vidal, A., Canals, M., and Acuña, J. L.: Seasonal pathways of organic matter within the Avilés submarine canyon: Food web implications, *Deep-Sea Res. Pt. I*, 117, 1–10, <https://doi.org/10.1016/j.dsr.2016.09.003>, 2016.
- Rumolo, P., Barra, M., Gherardi, S., Marsella, E., and Sprovieri, M.: Stable isotopes and C/N ratios in marine sediments as a tool for discriminating anthropogenic impact, *J. Environ. Monit.*, 13, 3399, <https://doi.org/10.1039/c1em10568j>, 2011.
- Salvadó, J. A., Grimalt, J. O., López, J. F., Palanques, A., Heussner, S., Pasqual, C., Sanchez-Vidal, A., and Canals, M.: Transfer of lipid molecules and polycyclic aromatic hydrocarbons to open marine waters by dense water cascading events, *Prog. Oceanogr.*, 159, 178–194, <https://doi.org/10.1016/j.pocean.2017.10.002>, 2017.
- Sanchez-Cabeza, J. A., Masqué, P., Ani-Ragolta, I., Merino, J., Frignani, M., Alvisi, F., Palanques, A., and Puig, P.: Sediment accumulation rates in the southern Barcelona continental margin (NW Mediterranean Sea) derived from  $^{210}\text{Pb}$  and  $^{137}\text{Cs}$  chronology, *Prog. Oceanogr.*, 44, 313–332, [https://doi.org/10.1016/S0079-6611\(99\)00031-2](https://doi.org/10.1016/S0079-6611(99)00031-2), 1999.
- Sanchez-Vidal, A., Higuera, M., Martí, E., Lique, C., Calafat, A., Kerhervé, P., and Canals, M.: Riverine transport of terrestrial organic matter to the North Catalan margin, NW Mediterranean Sea, *Prog. Oceanogr.*, 118, 71–80, <https://doi.org/10.1016/j.pocean.2013.07.020>, 2013.
- Sinninghe Damsté, J. S.: Spatial heterogeneity of sources of branched tetraethers in shelf systems: The geochemistry of tetraethers in the Berau River delta (Kalimantan, Indonesia), *Geochim. Cosmochim. Ac.*, 186, 13–31, <https://doi.org/10.1016/j.gca.2016.04.033>, 2016.
- Sinninghe Damsté, J. S., Hopmans, E. C., Pancost, R. D., Schouten, S., and Geenevasen, J. A. J.: Newly discovered non-isoprenoid glycerol dialkyl glycerol tetraether lipids in sediments, *Chem. Commun.*, 1683–1684, <https://doi.org/10.1039/b004517i>, 2000.
- Sinninghe Damsté, J. S., Schouten, S., Hopmans, E. C., van Duin, A. C. T., and Geenevasen, J. A. J.: Crenarchaeol: The characteristic core glycerol dibiphytanyl glycerol tetraether membrane lipid of cosmopolitan pelagic crenarchaeota, *J. Lipid Res.*, 43, 1641–1651, <https://doi.org/10.1194/jlr.M200148-JLR200>, 2002.
- Soru, S., Stipcich, P., Ceccherelli, G., Ennas, C., Moccia, D., and Pusceddu, A.: Effects of Field Simulated Marine Heatwaves on Sedimentary Organic Matter Quantity, Biochemical Composition, and Degradation Rates, *Biology (Basel)*, 11, 841, <https://doi.org/10.3390/biology11060841>, 2022.
- Soru, S., Berlino, M., Sarà, G., Mangano, M. C., De Vittor, C., and Pusceddu, A.: Effects of acidification on the biogeochemistry of unvegetated and seagrass marine sediments, *Mar. Pollut. Bull.*, 199, 115983, <https://doi.org/10.1016/j.marpolbul.2023.115983>, 2024.
- Stock, B. C., Jackson, A. L., Ward, E. J., Parnell, A. C., Phillips, D. L., and Semmens, B. X.: Analyzing mixing systems using a new generation of Bayesian tracer mixing models, *PeerJ*, 6, e5096, <https://doi.org/10.7717/peerj.5096>, 2018.
- Stuiver, M. and Polach, H. A.: Discussion Reporting of  $^{14}\text{C}$  Data, *Radiocarbon*, 19, 355–363, <https://doi.org/10.1017/S0033822200003672>, 1977.
- Tao, S., Eglinton, T. I., Montluçon, D. B., McIntyre, C., and Zhao, M.: Diverse origins and pre-depositional histories of organic matter in contemporary Chinese marginal sea sediments, *Geochim. Cosmochim. Ac.*, 191, 70–88, <https://doi.org/10.1016/j.gca.2016.07.019>, 2016.
- Tesi, T., Langone, L., Goñi, M. A., Wheatcroft, R. A., Miserocchi, S., and Bertotti, L.: Early diagenesis of recently deposited organic matter: A 9-yr time-series study of a flood deposit, *Geochim. Cosmochim. Ac.*, 83, 19–36, <https://doi.org/10.1016/j.gca.2011.12.026>, 2012.
- Tesi, T., Langone, L., Goñi, M. A., Turchetto, M., Miserocchi, S., and Boldrin, A.: Source and composition of organic matter in the Bari canyon (Italy): Dense water cascading versus particulate export from the upper ocean, *Deep-Sea Res. Pt. I*, 55, 813–831, <https://doi.org/10.1016/j.dsr.2008.03.007>, 2008.
- Thornton, S. F. and McManus, J.: Application of Organic Carbon and Nitrogen Stable Isotope and C/N Ratios as Source Indicators of Organic Matter Provenance in Estuarine Systems: Evidence from the Tay Estuary, Scotland, *Estuar. Coast. Shelf Sci.*, 38, 219–233, <https://doi.org/10.1006/ecss.1994.1015>, 1994.
- Tiano, J., De Borger, E., Paradis, S., Bradshaw, C., Morys, C., Pusceddu, A., Ennas, C., Soetaert, K., Puig, P., Masqué, P., and Sciberras, M.: Global meta-analysis of demersal fishing impacts on organic carbon and associated biogeochemistry, *Fish Fish.*, <https://doi.org/10.1111/faf.12855>, 2024.
- Tolosa, I., Fiorini, S., Gasser, B., Martín, J., and Miquel, J. C.: Carbon sources in suspended particles and surface sediments from the Beaufort Sea revealed by molecular lipid biomarkers and compound-specific isotope analysis, *Biogeosciences*, 10, 2061–2087, <https://doi.org/10.5194/bg-10-2061-2013>, 2013.
- Tranchina, L., Basile, S., Brai, M., Caruso, A., Cosentino, C., and Micciché, S.: Distribution of Heavy Metals in Marine Sediments of Palermo Gulf (Sicily, Italy), *Water. Air. Soil Pollut.*, 191, 245–256, <https://doi.org/10.1007/s11270-008-9621-3>, 2008.
- Verwege, M.-T., Somes, C. J., Schartau, M., Tuerena, R. E., Lorrain, A., Oschlies, A., and Slawig, T.: Description of a global marine particulate organic carbon-13 isotope data set, *Earth Syst. Sci. Data*, 13, 4861–4880, <https://doi.org/10.5194/essd-13-4861-2021>, 2021.
- Viso, A.-C. and Marty, J.-C.: Fatty acids from 28 marine microalgae, *Phytochemistry*, 34, 1521–1533, [https://doi.org/10.1016/S0031-9422\(00\)90839-2](https://doi.org/10.1016/S0031-9422(00)90839-2), 1993.

- Volkman, J. K., Johns, R. B., Gillan, F. T., Perry, G. J., and Bavor, H. J.: Microbial lipids of an intertidal sediment – I. Fatty acids and hydrocarbons, *Geochim. Cosmochim. Ac.*, 44, 1133–1143, [https://doi.org/10.1016/0016-7037\(80\)90067-8](https://doi.org/10.1016/0016-7037(80)90067-8), 1980.
- Wakeham, S. G. and McNichol, A. P.: Transfer of organic carbon through marine water columns to sediments – insights from stable and radiocarbon isotopes of lipid biomarkers, *Biogeosciences*, 11, 6895–6914, <https://doi.org/10.5194/bg-11-6895-2014>, 2014.
- Wang, X., Zhang, Y., Luo, M., Xiao, K., Wang, Q., Tian, Y., Qiu, W., Xiong, Y., Zheng, C., and Li, H.: Radium and nitrogen isotopes tracing fluxes and sources of submarine groundwater discharge driven nitrate in an urbanized coastal area, *Sci. Total Environ.*, 763, 144616, <https://doi.org/10.1016/j.scitotenv.2020.144616>, 2021.
- Wei, B., Kusch, S., Wu, J., Shaari, H., Mollenhauer, G., and Jia, G.: River mouths are hotspots for terrestrial organic carbon burial on the Sunda Shelf: Implications for tropical coastal carbon sequestration, *Geochim. Cosmochim. Ac.*, 387, 1–11, <https://doi.org/10.1016/j.gca.2024.10.037>, 2024.
- Wei, B., Müller, D., Kusch, S., Niu, L., Hefter, J., Sander, L., Hanz, U., Mollenhauer, G., Jia, G., Kasten, S., and Holtappels, M.: Twice the global average carbon burial efficiency in the Helgoland Mud Area of the North Sea: Insights into carbon sequestration in small-size depocenters on sand-dominated shelves, *Chem. Geol.*, 681, 122712, <https://doi.org/10.1016/j.chemgeo.2025.122712>, 2025.
- Weijers, J. W. H., Schefuß, E., Kim, J.-H., Sinninghe Damsté, J. S., and Schouten, S.: Constraints on the sources of branched tetraether membrane lipids in distal marine sediments, *Org. Geochem.*, 72, 14–22, <https://doi.org/10.1016/j.orggeochem.2014.04.011>, 2014.
- Xiao, W., Wang, Y., Zhou, S., Hu, L., Yang, H., and Xu, Y.: Ubiquitous production of branched glycerol dialkyl glycerol tetraethers (brGDGTs) in global marine environments: a new source indicator for brGDGTs, *Biogeosciences*, 13, 5883–5894, <https://doi.org/10.5194/bg-13-5883-2016>, 2016.
- Yedema, Y. W., Sangiorgi, F., Sluijs, A., Sinninghe Damsté, J. S., and Peterse, F.: The dispersal of fluvially discharged and marine, shelf-produced particulate organic matter in the northern Gulf of Mexico, *Biogeosciences*, 20, 663–686, <https://doi.org/10.5194/bg-20-663-2023>, 2023.
- Zhu, C., Wagner, T., Pan, J.-M., and Pancost, R. D.: Multiple sources and extensive degradation of terrestrial sedimentary organic matter across an energetic, wide continental shelf, *Geochem. Geophys. Geosy.*, 12, <https://doi.org/10.1029/2011GC003506>, 2011.